Imperial College London
Department of Theoretical Physics

The Backflow Effect

Author:
James Sprinz

Supervisor:
Professor Jonathan Halliwell

Submitted in partial fullfillment of the requirements for the degree of Master of Science of Imperial College London

20^{th} September 2013

Abstract

We investigate backflow — the remarkable effect during which a particle's probability travels in the opposite direction to its momentum. We present an extensive review of the relevant literature and discuss many aspects of the phenomenon as well as providing suggestions for further lines of study. The effect is related to may of the conceptual issues surrounding time and is therefore relevant to understanding the foundations of quantum mechanics.

Acknowledgements

Many thanks go to my supervisor Jonathan Halliwell for all his help with this project. I have really enjoyed learning about the backflow effect and spending time investigating some of the foundational issues of quantum mechanics involving time.

Contents

1. Introduction

Imagine a 1-dimensional free particle located in $x < 0$ which has only positive momentum components; it seems obvious that at all times the probability that the particle will be found in $x > 0$ is monotonically increasing. Remarkably, in quantum mechanics this is not the case. There are states for which the probability that the particle stays in $x < 0$ temporarily increases because the probability current $J(x, t)$ is negative and opposes the direction of momentum. This strange effect is called backflow.

It was first discovered in 1969 by Allcock [1] in connection with his seminal works on the arrival-time problem in quantum mechanics [2, 3]. Interest in backflow then lay dormant for more than 20 years until it was rediscovered by Bracken and Melloy [4] who explicitly studied and described many of its features. They calculated a least upper bound, c_{bm}, for the amount of probability that can 'flow back' during a given interval. They obtained a value of 0.04 and surprisingly discovered that this bound is a dimensionless constant independent of any parameters, in particular $\hbar$. It was declared to be "a new quantum number".

Since then interest in the subject has increased and various authors have investigated features of the effect. Eveson et al [5] and Penz et al [6] improved Bracken and Melloy's calculation to obtain a more accurate value for c_{bm}. Penz et al also worked on finding a backflow maximising state — a state whose negative flux approaches c_{bm} — and were able to do so with numerical calculations. There has been some success with approximating this state using analytic functions but so far no state has been found which matches the full backflow behaviour [7]. Bracken and Melloy investigated the cases of backflow

in opposition to a force and for a relativistic Dirac particle [8, 9]. They found that these extra features of the system introduced parameter dependence into the maximum flux. Recently, a new type of backflow has been discovered in which the effective angular momentum is directed in opposition to that of the wavefunction's components; in contrast to other examples of backflow, this effect can last indefinitely [10].

Muga et al investigated the relation between backflow and detectors, noting that the effect requires us to change our classical definition of a perfectly absorbing detector [11]. Their paper also discussed the relationship between backflow and the arrival-time problem [11–19], a connection which has been acknowledged by various authors. In trying to find an experimental method for verifying the effect, a range of detector models have been discussed and Yearsley et al showed that providing a realistic model for backflow can introduce a classical limit [7]. A very recent proposal by Palmero et al [20] provides a detailed method for experimentally verifying the backflow effect. It is hoped that this experiment will be conducted soon so that many of the subject's open questions can be answered.

A wide variety of states can produce backflow but all require superposition. Plane waves yielded small amounts of backflow, which led Yearsley et al to investigate superpositions of Gaussians instead [21]. These attained higher levels of negative flux but still only around 16% of the theoretical maximum. Recently, Halliwell et al [22] discovered an exhaustive class of backflow states and, using a particular Gaussian example, achieved a negative flux which was 41% of the maximum.

Using their newly discovered bound, Bracken and Melloy were able to provide a temporal limit on the backflow effect [4]. Their limit bounds the product of the current and its duration, so that one can have arbitrarily negative current but for extremely short times. Similarly, Eveson et al discovered a spatial bound which limits the product of the backflow area and the current [5]. It remains an open question whether any other bounds exist and, if so, what they are. Berry [23] took a new approach to the backflow problem and attempted to measure what fraction of the x-axis is undergoing backflow, thereby deriv-

ing a probability that the particle will be in one of those regions. He also introduced the connection with superoscillations, another remarkable quantum effect [24–26].

Backflow raises the intriguing possibility of introducing negative probabilities [27, 28] and invites discussion of Bohmian theory, particularly with reference to the arrival-time problem [29]. Time is an oft debated topic in quantum mechanics because no classical notion of time transitions smoothly to the quantum world [14, 30]. Backflow inherits the contentions of time and provides no obvious way to explain the effect. It is, however, generally accepted that backflow results from interference between parts of the wavepacket — which is indicated by the requirement that its Wigner function be negative [4, 7] — and hidden structure within the Heisenberg uncertainty relations [10].

In this paper we will attempt a complete review of the subject. The details of the effect and how it occurs will be described along with the variety of states for which it obtains. We will investigate detection methods and how a negative probability can reveal itself in a positive recording. There is still relatively little known about backflow and it is our hope that this paper will provide the reader with most of the details as well as suggesting some further ideas for investigation.

2. The backflow effect

2.1 Probability, the current and the flux

Consider a non-relativistic spinless free particle described by a wavefunction $\psi(x,t)$ with positive momentum components only, localised in $x<0$[1]. The particle's probability density is,

$$\rho(x,t)=\psi(x,t)\psi^*(x,t)=|\psi(x,t)|^2 \tag{2.1}$$

and its probability current is,

$$J(x,t)=-\frac{i\hbar}{2m}\left[\psi^*(x,t)\frac{\partial\psi(x,t)}{\partial x}-\frac{\partial\psi^*(x,t)}{\partial x}\psi(x,t)\right], \tag{2.2}$$

where m is the mass of the particle. The probability density and current obey the continuity equation,

$$\frac{\partial J(x,t)}{\partial x}+\frac{\partial\rho(x,t)}{\partial t}=0 \tag{2.3}$$

which expresses quantum mechanical conservation of probability.

The probability that the particle is located within a region $[x_a,x_b]$ at time t is simply the spatial integral of the probability density over this region,

$$P(t)=\int_{x_a}^{x_b}\rho(x,t)\,\mathrm{d}x\,. \tag{2.4}$$

[1]The particle cannot be perfectly localised in this region and at the same time have definite positive momenta since these two properties do not commute. Instead we can consider the particle to be strongly concentrated in $x<0$.

We can use this to derive an expression for the probability flux, which is the change in probability in a region over time. For example, the probability flux across the origin, $x = 0$, during the interval $[t_1, t_2]$ is,

$$\begin{aligned} F(t_1, t_2) &= \int_{-\infty}^{0} \rho(x, t_1)\, \mathrm{d}x - \int_{-\infty}^{0} \rho(x, t_2)\, \mathrm{d}x \\ &= P(t_1) - P(t_2) \qquad (2.5) \\ &= \int_{t_1}^{t_2} J(0, t)\, \mathrm{d}t \qquad (2.6) \end{aligned}$$

We see that the flux can equivalently be defined as the total amount of current flowing out of a region during the time interval. Assuming that $J(-\infty, t) = 0$, then using (2.3) and (2.4) one finds,

$$\frac{\mathrm{d}P(t)}{\mathrm{d}t} = -J(0, t)\,. \qquad (2.7)$$

This equation illustrates why backflow is a quantum effect. Classically for a particle with positive momentum $J(0, t) \geq 0 \ \forall t > 0$ so the probability that the particle is located in $[-\infty, 0]$ must decrease monotonically with time[2]. In contrast, quantum mechanics allows $J(0, t)$ to take negative values even though all component momenta are positive, which results in $P(t)$ increasing with time. In this situation the current is flowing in opposition to the positive momentum, resulting in a temporary increase in the probability of finding the particle in the negative region of the x-axis.

2.2 Operators

In order to study the backflow effect it is helpful to rewrite the above equations in terms of quantum mechanical operators. By writing equations (2.5) and (2.6) in this way we can find the flux operator's eigenstates and study its spectrum. Bracken and Melloy used this method [4] to find an upper bound on the amount of probability that can flow backwards

[2]Strictly it cannot increase with time, taking into account the possibility that $J(0, t) = 0$.

which will be repeated below. First we define the current,

$$\hat{J}(t) = \frac{1}{2m}[\hat{p}\delta(\hat{x}) + \delta(\hat{x})\hat{p}], \tag{2.8}$$

where $\hat{p}$ and $\delta(\hat{x})$ are the usual quantum mechanical momentum and position operators respectively. Using the Heaviside step function θ we construct a projection operator onto the positive x-axis, $\hat{P} = \theta(\hat{x})$, and its counterpart onto the negative x-axis, $\bar{P} = 1 - \theta(\hat{x}) = \theta(-\hat{x})$, which define the flux operator

$$\hat{F}(t_1, t_2) = \bar{P}(t_1) - \bar{P}(t_2) = \hat{P}(t_2) - \hat{P}(t_1) \tag{2.9}$$

$$= \int_{t_1}^{t_2} \hat{J}(t)\, \mathrm{d}t. \tag{2.10}$$

Penz et al [6] have rigorously studied this flux operator and shown that it is linear bounded, self-adjoint, and non-compact. The flux is naturally interpreted as the expectation value of its operator and equations (2.5) and (2.6) can be rewritten as,

$$\begin{aligned} F(t_1, t_2) &= \langle \hat{F}(t_1, t_2) \rangle \\ &= \langle \bar{P}(t_1) \rangle - \langle \bar{P}(t_2) \rangle \\ &= \int_{t_1}^{t_2} \langle \psi | \hat{J}(t) | \psi \rangle \ \mathrm{d}t. \end{aligned} \tag{2.11}$$

In the last line we have expressed the relation between the current and its operator, $J(t) = \langle \psi | \hat{J}(t) | \psi \rangle$. Quantum mechanically $J(0, t)$ can be negative which means that $\hat{J}(t)$ cannot be a positive operator. A clue to this negativity lies in its construction. $\hat{J}(t)$ is composed of the position and momentum operators which are both non-negative operators on states with definite positive momentum. However, they do not commute, which allows $\hat{J}$ to be negative [7]; this has led some authors to suggest that backflow is "ultimately a demonstration of the effects of the uncertainty principle" [10, p.2]. Positive operators are requisite in quantum mechanics due to its probabilistic nature. A negative expectation value can imply a negative probability, a contentious concept which will be discussed in section 8.

Taking this view, one could interpret a negative current as the positive flow of negative probability instead of probability backflow.

With the operators defined, it is now possible to study the spectrum of the flux operator and find an upper bound on the maximum amount of probability backflow. It is to this problem that we will turn in the next section.

2.3 The eigenvalue equation

We can investigate features of the backflow effect by studying the spectrum of the flux operator and finding a solution to the following eigenvalue equation,

$$\theta(\hat{p})\hat{F}(t_1, t_2)\,|\phi\rangle = \lambda\,|\phi\rangle\,, \tag{2.12}$$

where the states $|\phi\rangle$ consist of positive momenta only. In the following derivation, we follow Yearsley [7] and use an opposite sign convention to Bracken and Melloy [4]. Hence, backflow states are ones in which $\lambda < 0$ and the most negative eigenvalue will be equivalent to Bracken and Melloy's upper bound. We rewrite the time interval $[t_1, t_2]$ as $[-T/2, T/2]$ for convenience and then express (2.12) in momentum space as,

$$\frac{1}{\pi}\int_0^\infty \frac{\sin(T[p^2 - q^2]/4m\hbar)}{p - q}\phi(q)\,\mathrm{d}q = \lambda\phi(p). \tag{2.13}$$

This can be written in a simpler, compact form by expressing p and q in terms of the new variables u and v:

$$p = 2\sqrt{m\hbar/T}u \qquad q = 2v\sqrt{m\hbar/T} \tag{2.14}$$

$$\frac{1}{\pi}\int_0^\infty \frac{\sin(u^2 - v^2)}{u - v}\varphi(v)\,\mathrm{d}v = \lambda\varphi(u), \tag{2.15}$$

where $\varphi(u) = [m\hbar/4T]^{1/4}\phi(p)$ is the rescaled dimensionless wavefunction. Equation (2.15) is clearly independent of all physical parameters $\hbar$, m and T, so the eigenvalues are both dimensionless and independent of parameters. Having rescaled the wavefunction, the

flux in terms of these new variables is,

$$F(-T/2, T/2) = \frac{1}{\pi}\int_0^\infty \mathrm{d}u \int_0^\infty \varphi^*(u)\frac{\sin(u^2 - v^2)}{u - v}\varphi(u)\,\mathrm{d}v. \tag{2.16}$$

What is the spectrum of Eqn.(2.15)? It is a real equation which therefore has real-valued eigenstates and eigenvalues. Evidently λ must take values close to 1 for wavepackets which entirely crossed the origin within the time interval and values approximating 0 for those that have not crossed at all. So we see that the eigenvalues must lie in the range,

$$-\,c_{bm} \leq \lambda \leq 1\,, \tag{2.17}$$

where c_{bm} is the least upper bound on the amount of backflow, first computed by Bracken and Melloy [4]. Backflow maximising states — eigenstates of Eqn.(2.15) which produce the greatest negative flux — will have eigenvalues approaching c_{bm}. As of yet Eqn.(2.15) has not be solved analytically and Bracken and Melloy numerically computed an initial value of $c_{bm} \approx 0.04$. This has since been improved by various authors [5, 6] and the currently accepted value is that of Penz et al, $c_{bm} \approx 0.038452$. Since the result c_{bm} is independent of the choice of state we can assume that it is a universal constant, valid for any state described by quantum mechanics, which led Bracken and Melloy to label c_{bm} 'a new quantum number'.

3. The limits of backflow

3.1 The new quantum number

The bound c_{bm} of Bracken and Melloy is worth looking at closely for it reveals some interesting features about the backflow effect. Clearly, a bound of some kind should be expected. Were there to be no limit, then the probability of finding the particle in the region $x < 0$ could approach unity. Whilst the backflow effect is already counter-intuitive, an unlimited backflow effect is simply implausible. It would indicate a breakdown in the quantum mechanical description for states to exist which could be located with certainty in the opposite direction to which they travel.

Of immediate note is the independence of c_{bm} of any parameter at all. In particular, the independence of T suggests that the effect can last indefinitely. Using (2.6) we see that this is almost correct: backflow can last for arbitrary lengths of time as long as the total flux is bounded from below,

$$\int_{-T/2}^{T/2} J(t)\,\mathrm{d}t \geq -c_{bm}\,, \tag{3.1}$$

which leads to,

$$TJ(\chi) \geq -c_{bm}\,, \tag{3.2}$$

where χ is any time in the interval $[-T/2, T/2]$. So one could have states with arbitrarily large negative current for brief moments of time or, alternatively, states with tiny amounts of negative current for lengthy amounts of time.

The lack of time dependence is not c_{bm}'s only interesting feature: its independence of $\hbar$

is also somewhat remarkable. One usually tries to restore the classical limit of a quantum effect by letting $\hbar \to 0$, which is clearly not possible in the present case and begs the question: how does the effect disappear classically? We know that classical backflow doesn't exist yet there seems to be no clear way for the effect to vanish on a classical scale. This issue will be discussed in detail in section 6.

3.2 A spatial bound

The existence of a bound on the total *amount* of probability which can flow back naturally leads one to enquire whether any other backflow bounds exist. Eveson et al [5] answered this question in the affirmative. Based on work in quantum field theory (QFT) they proved that there is an inequality which limits the spatial extent of backflow. Similar to Eqn.(3.1), which relates duration of the backflow effect to the strength of the current, one can have arbitrarily negative currents if only in sufficiently small regions of space.

In QFT, it is possible for the renormalised energy density of the field to assume a negative value; in fact, the energy density can be made arbitrarily negative by a particular choice of state. Evidence for this effect has been found between Casimir plates indirectly by experiment [31]. However, this remarkable and counterintuitive feature of QFT is strictly limited by quantum weak energy inequalities (QWEIs). These limit the magnitude and duration of negative energy densities at a particular spacetime point. Eveson et al saw a similarity between the counterintuitive features of negative energy and those of backflow, which led them to speculate that there may be similar inequalities which apply to backflow.

Eveson et al start by demonstrating the similarity between backflow and negative energy density. In particular, they show that the probability current can be made arbitrarily negative by a suitable choice of state, which includes a 'tuning' parameter k_0 in the normalisation constant. They note that Bracken and Melloy's bound is an inequality of the

form,

$$P(t) \leq P(0) + c_{bm}\,, \tag{3.3}$$

where $P(t)$ is the probability of finding the particle in the region $x < 0$. This inequality is clearly dependent on time which, Eveson et al argue, demonstrates 'the transitory nature' of backflow [5, p. 5]. In contrast, their bound limits the spatial extent of backflow.

Their proof starts by considering spatially smeared quantities,

$$J(f) = \int J(x) f(x)\, \mathrm{d}x\,, \tag{3.4}$$

where $J(f)$ is the instantaneous probability current measured by an extended detector and $f(x)$ is any smooth, complex-valued function with compact support. Note that we have removed the time dependence from J as we are considering instantaneous snapshots of the current. It is useful to express the current in a different form from Eqn.(2.2),

$$J(x) = \frac{\mathrm{Re}\,\overline{\psi(x)}[\hat{p}\psi(x)]}{m}, \tag{3.5}$$

over which we can spatially integrate to find an expectation value for the velocity,

$$\int J(x)\,\mathrm{d}x = \frac{\mathrm{Re}\,\langle\psi|\hat{p}|\psi\rangle}{m} = \frac{\langle\hat{p}\rangle}{m}\,. \tag{3.6}$$

Combining Eqn.(3.4) and (3.6) we get,

$$\int J(x) f(x)\,\mathrm{d}x = \frac{1}{m}\mathrm{Re}\,\langle\psi(x)|f(x)\hat{p}|\psi(x)\rangle \tag{3.7}$$

and we then transform the right hand side to momentum space,

$$\int J(x) f(x)\,\mathrm{d}x = \frac{\hbar}{m}\int \frac{k}{2\pi}\,|g(k)\psi(k)|^2\,\mathrm{d}k\,. \tag{3.8}$$

By estimating the portion of the integral originating in $k < 0$ we derive a bound on

Eqn.(3.8),

$$\int J(x)f(x)\,\mathrm{d}x \geq \frac{\hbar}{m}\int_{-\infty}^{0}\frac{k}{2\pi}\left|g(k)\psi(k)\right|^2\,\mathrm{d}k = -\frac{\hbar}{m}\int_{-\infty}^{0}\frac{k}{2\pi}\left|g(-k)\psi(-k)\right|^2\,\mathrm{d}k \tag{3.9}$$

The convolution theorem states,

$$g(k)\psi(k) = \frac{1}{2\pi}\int_0^\infty \psi(k')g(k-k')\,\mathrm{d}k'\,. \tag{3.10}$$

Since g is real valued, $|g(n)|^2 = |g(-n)|^2$ and using the Cauchy-Schwarz inequality,

$$|g(-k)\psi(-k)|^2 \leq \frac{1}{2\pi}\int_0^\infty |g(k+k')|^2\mathrm{d}k'\,. \tag{3.11}$$

Now, substituting this back into Eqn.(3.9), we can derive the full inequality.

$$\begin{aligned}\int J(x)f(x)\,\mathrm{d}x &\geq -\frac{\hbar}{m}\int_0^\infty \frac{\mathrm{d}k}{2\pi}\int_0^\infty \frac{k}{2\pi}|g(k+k')|^2\,\mathrm{d}k' \\ &= -\frac{\hbar}{8\pi m}\int |g'(x)|^2\mathrm{d}x\end{aligned} \tag{3.12}$$

where we have set $f(x) = g(x)^2$ and used Parseval's theorem. Note that this proof applies only to the class of normalised wavefunctions $\mathfrak{R}$ which satisfy,

$$\mathfrak{R} = \{\psi \in L^2(\mathbb{R}) : \psi(k) = 0 \text{ for } k < 0\}\,. \tag{3.13}$$

The inequality (3.12) has a number of interesting features which we will discuss. Firstly, there is no upper bound on the smeared flux which we show with the following substitution. Let $\psi_\alpha(x) = e^{i\alpha x}\psi(x)$, then our expression for the current becomes,

$$J_\alpha(x) = J(x) + \frac{\alpha\hbar}{m}|\psi(x)|^2 \tag{3.14}$$

from which we can clearly see that

$$\int J_\alpha(x) f(x)\, \mathrm{d}x \to \infty \;\text{ as }\; \alpha \to \infty\,. \tag{3.15}$$

Hence, the current can grow in strength indefinitely in any region of the x-axis; spatial limits do not exist for positive current.

Secondly, we see that the inequality provides a bound on the product of the negative flux times the square of its spatial extent. The scaling of this bound is understood by setting $f(x) \to f_\alpha(x) = \alpha^{-1/2} f(x/\alpha)$, which makes the right hand side of the the inequality (3.12) scale by a factor α^{-2}. In the limit $\alpha \to 0$ the right hand side of Eqn.(3.12) blows up, demonstrating that the current is unbounded from below (i.e., it can be arbitrarily negative in a point-like region). The limit $\alpha \to \infty$ makes the inequality vanish which is congruous with the fact that $\langle \hat{p} \rangle \geq 0$ and hence no bound obtains.

Thirdly, as with the bound c_{bm}, the entire proof is state-independent and hence universally applicable. But, in contrast to Bracken and Melloy's bound [4], this inequality is kinematical, not dynamical. The proof was independent of a choice of Hamiltonian so the bound is a feature of backflow itself, rather than of any particular system exhibiting the effect.

Finally, we see that both $\hbar$ and m are featured within the inequality (3.12) which allows us to restore the classical limit either by letting $\hbar \to 0$ or in the limit of large mass.

What other inequalities exist which limit the backflow effect? There are a variety of possibilities which are yet to be explored. Immediately, a spacetime inequality springs to mind: instead of two separate inequalities setting bounds on the temporal and spatial extent of backflow, perhaps there is one which unifies these two; i.e., the negativity of the current is limited by the volume of a spacetime region. Inequalities of a different sort, perhaps relating the magnitude of the momentum to the negativity of the current or the frequency with which separate backflow instances can occur, might exist. As with most issues surrounding backflow, there is a great deal of work to be done and many directions

remain unexplored. In the next section we look at an attempt to measure the spatial extent of backflow and quantify what portion of the x-axis is undergoing the effect.

3.3 Measuring backflow

In a recent paper [23] Berry takes a very different approach from previous efforts to understand backflow. His aim is to quantify what portion of the x-axis may be undergoing backflow and, therefore, work out the probability that the particle or wavepacket will be located in a back-flowing region. Berry also defines backflow in a different way to previous authors. Instead of focusing on the current $J(x,t)$ and whether this assumes negative values, he looks instead at the local phase gradient of the wavefunction whose sign indicates whether the wave is locally travelling forwards or backwards. Restricting the wavefunction to consist of only positive wavenumbers ensures that globally the wave is always travelling forwards. However, this requirement doesn't negate the possibility that the *local* wavenumber is negative and the wavepacket is exhibiting backflow. This alternative formulation of backflow is not only useful for Berry's work but is helpful in gaining insight into the effect and will be discussed further in section 8.

The key to Berry's analysis is to write the wavefunction, ψ, in the phase-amplitude form. Rather than expressing ψ as a superposition of positive momentum plane waves,

$$\psi(x) = \sum_{n=0}^{N} c_n e^{ik_n x} \,, \tag{3.16}$$

where $k_n \geq 0$ are the wavenumbers of the respective plane waves. We instead write ψ in the following way,

$$\psi(x) = \alpha(x) \text{exp}\left[i \int_0^x k(x') \, \mathrm{d}x' \right] \,, \tag{3.17}$$

where both the amplitude $\alpha(x)$ and the local wavenumber,

$$k(x) = \partial_x \arg \psi(x) = \text{Im} \frac{\partial_x \psi(x)}{\psi(x)}\,, \tag{3.18}$$

are real. When $k(x) > 0$ the wave is locally travelling forwards and when $k(x) < 0$ the wave is locally travelling backwards; the latter case is backflow. Berry shows with various wavefunctions that it is easy to set up situations in which $k(x) < 0$.

Before we proceed further, it is necessary to introduce the notion of weak measurement. Weak measurements were first proposed by Aharanov et al [32] in 1988 as a method of measurement which doesn't disturb the system being measured. This is achieved by making the coupling between the measuring device and the system sufficiently weak; however, the price for not disturbing the system is greater error in the result[3][33]. The 'weak values' that result from such measurements are often remarkably surprising, bordering on non-physical. It has been shown that weak measurements can return values of negative kinetic energy [34] , speeds of a charged particle greater than the speed of light [35] and values far outside the spectrum of the observable's eigenvalues [32]. Amongst this company, backflow no longer seems so bizarre.

A weak measurement depends on the system's preselected as well as postselected states $|\psi\rangle$ and $|\phi\rangle$ respectively. So for some observable A, its weak value is given by,

$$A_{\text{weak}} = \frac{\langle \phi | \hat{A} | \psi \rangle}{\langle \phi | \psi \rangle} \tag{3.19}$$

where $|\psi\rangle$ and $|\phi\rangle$ can be any non-orthogonal states. Weak measurement allows one to measure non-commuting observables. However, as the above examples demonstrate, the results may not be as expected or particularly useful, so some care must be taken in interpreting the results of a weak measurement. The connection with backflow should now be becoming clear. It was mentioned in section 2 that backflow in some sense originates

[3]Individual readings of the weak measuring device may contain large errors but repetition of the experiment necessarily reduces this error allowing us to achieve measurements with as much precision as we like.

in the non-commutativity of position and momentum, which allows the current to take negative values. It is possible that a weak measurement of the momentum could lead to a negative result.

A weak measurement of the momentum on the preselected state $|\psi\rangle$ with position $|x\rangle$ postselected yields the local wavenumber up to a factor $\hbar$ [23],

$$p_{\text{weak}} = \text{Re}\frac{\langle x|\hat{p}|\psi\rangle}{\langle x|\psi\rangle} = k(x)\,. \tag{3.20}$$

In some sense we can regard $k(x)$ as the local expectation value of the momentum; when this expectation value is negative then backflow occurs.

Berry has derived a function for calculating the fraction of the axis in which $k(x) < 0$ [23], which he calls the backflow probability P_b,

$$\begin{aligned} P_b &= \lim_{L\to\infty} \frac{1}{2L}\int_{-L}^{L} \theta(-k(x))\,\mathrm{d}x \\ &= \int_{-\infty}^{0} \rho_k(k)\,\mathrm{d}k\,, \end{aligned} \tag{3.21}$$

where ρ_k is the probability density of the local wavenumber,

$$\rho_k(k) = \lim_{L\to\infty} \frac{1}{2L}\int_{-L}^{L} \delta(k - k(x))\,\mathrm{d}x\,. \tag{3.22}$$

P_b is a measure of what fraction of the x-axis is undergoing backflow, it should not be confused with the amount of probability that actually flows back when the probability current is negative. We would expect that P_b is limited in some respect by the spatial inequality (3.12).

An operator $\hat{A}$ with eigenvalues A_n symmetrically distributed in the range $-A_{\text{max}} \leq A_n \leq +A_n$ has a probability distribution of weak values, A_{weak}. When the pre and postselected states are randomly chosen this distribution takes the form

$$\rho(A_{\text{weak}}) = \frac{\langle A_n^2\rangle}{2[A_{\text{weak}}^2 + \langle A_n^2\rangle]^{3/2}}\,, \tag{3.23}$$

where here, and for the rest of this section, $\langle ... \rangle$ denotes an ensemble average rather than a quantum mechanical expectation value. We consider only positive semi-definite wave numbers by specifying $A_{\text{weak}} = -A_{\text{max}} + k$ and $A_n = -A_{\text{max}} + k_n$. Using Eqn.(3.23) to get a function for Eqn.(3.22), the wavenumber probability density, we input this to Eqn.(3.21) to get Berry's main result:

$$P_b = \frac{1 - r_b}{2} \tag{3.24}$$

where,

$$r_b \equiv \frac{\langle k_n \rangle}{\sqrt{\langle k_n^2 \rangle}} \tag{3.25}$$

Eqn.(3.25) reveals that the backflow probability Eqn.(3.24) depends on the distribution of the component momenta k_n. The larger the spread, the larger the back-flowing fraction of the x-axis. P_b nears its maximum value $1/2$ when $r_b = 0$ so $\langle k_n^2 \rangle \gg \langle k_n \rangle^2$. This is an important result which highlights the importance of component momenta in determining the extent of the backflow effect.

Berry demonstrates his findings on a variety of wave functions; in particular he uses a 20-wave superposition of the form (3.16) to produce a display of the backflow regions of the x-axis. These results are repeated here as they effectively delineate the relation between momenta and backflow regions. Using Eqn.(3.16) and inputting the following values,

$$N = 20, \quad k_n = n, \quad c_0 = 0, \quad c_{n>0} = \frac{1}{\sqrt{n}} e^{i\phi_n}, \tag{3.26}$$

where ϕ_n is a random phase factor from the interval $[0, 2\pi]$, we get the following wavefunction,

$$\psi(x) = \sum_{n=1}^{20} \frac{1}{\sqrt{n}} e^{i(nx + \phi_n)} \tag{3.27}$$

The wavefunction is 2π periodic in x and has a predicted probability value of $P_b = 0.136$. By plotting the local wavenumber we can actually measure the fraction of the axis for which backflow occurs; this is shown in Fig.(1). We see that there are 9 backflow regions in one period and their total measured extent is $P_b = 0.163$ which is a difference of ap-

proximately 16%. This is good agreement for such a small sample of backflow regions.

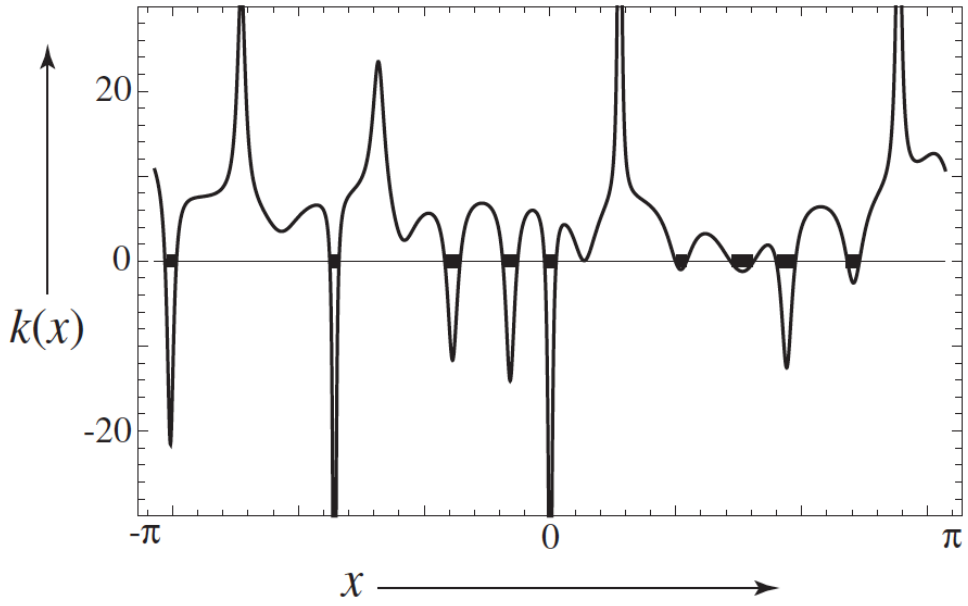

Figure 1: Local wavenumber $k(x)$ as a function of position for the 20-wave superposition (3.27). Backflow regions are shown with black bars [23].

We can investigate the relation between the current and the spatial extent of backflow by plotting the backflow regions for various values of negative $k(x)$. Using a simple two-wave superposition we can easily vary $k(x)$ and obtain the necessary results. Our wavefunction is,

$$\psi(x) = 1 - ae^{ix}\,, \tag{3.28}$$

which has a local wavenumber given by Eqn.(3.18),

$$k(x) = a\frac{a - \cos x}{1 + a^2 - 2a\cos x}\,. \tag{3.29}$$

This simple wavefunction exhibits backflow when $a < 1$ in the interval $|x| < \cos^{-1} a$. As a increases $k(x)$ becomes progressively negative but we see from Fig.(2) that the backflow region correspondingly decreases. This is precisely the relation predicted by Eveson's inequality (3.12), which bounded the extent of area in which there could be negative current. Berry has thus provided important evidence to support the conclusions of Eveson et al [5].

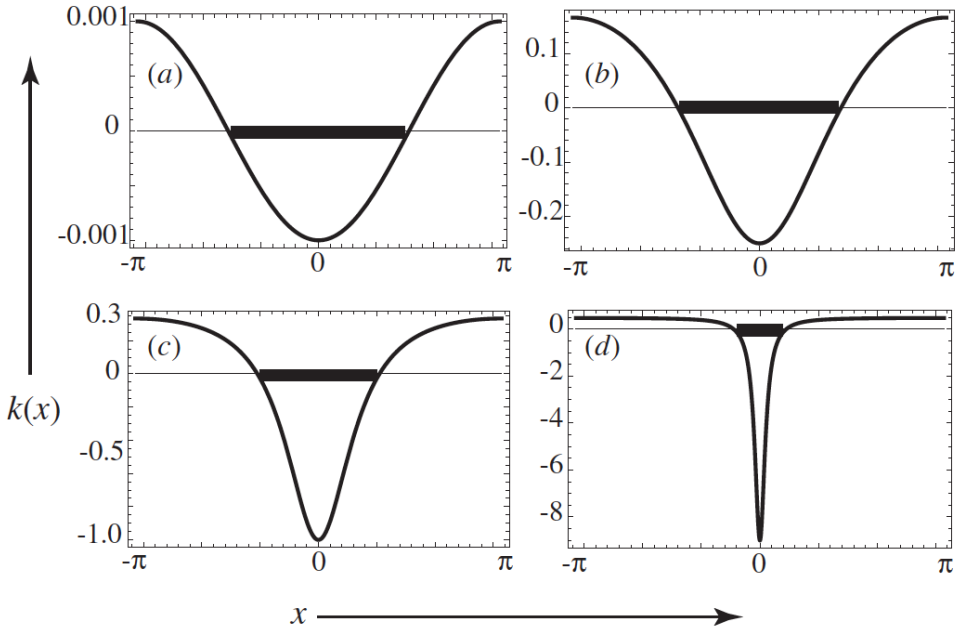

Figure 2: Local wavenumber k(x) for the two-wave superposition (3.28), with backflow regions shown by black bars, for (a) a = 0.001, (b) a = 0.2, (c) a = 0.5, (d) a =0.9. [23].

3.3.1 Strong backflow

We can generalise Eqn.(3.28) to write a superposition of plane waves as,

$$\psi(x) = [1 - ae^{ix}]^N \,, \tag{3.30}$$

where $N \gg 1$ and $a < 1$. This function is a variation of functions studied in the context of superoscillations [26], another quantum effect, which Berry relates to backflow. Superoscillations occur when waves locally oscillate at a far greater frequency than any of the components of their Fourier spectrum [24, 25]. The connection with backflow is obvious; both are paradoxical effects where a physical property of a state takes a local value outside the spectrum of its individual components. It is important to note that Eqn.(3.30) can be

made equivalent to Eqn.(3.16) simply by defining the parameters as follows,

$$\psi(x) = [1 - ae^{ix}]^N = \sum_{n=0}^{N} c_n e^{ik_n x} \tag{3.31}$$

if

$$c_n = (-a)^n \frac{N!}{n!(N-n)!} \qquad \text{and} \qquad k_n = n \tag{3.32}$$

We see that the phases of this wavefunction (3.30) are not random but are evenly distributed. No k_n are negative but using Eqn.(3.18), the local wavenumber at $x = 0$ takes the value,

$$k(0) = -\frac{Na}{1-a}\,, \tag{3.33}$$

which is clearly negative for $0 < a < 1$; this is an example of backflow. The power spectrum of $|c_n|^2$ is distinctly Gaussian and strongly peaked around $\langle k_n \rangle \approx Na/(1+a)$ which leaves the local wavenumber Eqn.(3.33) lying outside the spectrum. The backflow fraction of the x-axis is,

$$P_b = \frac{\cos^{-1} a}{\pi}\,, \tag{3.34}$$

which is significantly greater than that predicted by Eqn.(3.24),

$$P_b \approx \frac{1}{8Na}\,. \tag{3.35}$$

The reason is that Eqn.(3.24) predicts the backflow fraction based on the power spectrum with the assumption that the phases are random; however, for Eqn.(3.30) they are not. Berry calls this type of backflow, for which the phases are correlated and P_b is large, 'strong backflow' [23].

How do the backflow regions evolve over time? We would expect random superpositions like Eqn.(3.27) to approximately conserve P_b as it is based on the wavefunction's power spectrum, which is unchanged in time. In contrast, we should expect that "evolution soon destroys the delicate conspiracy of phases responsible for the strong backflow"

[23, p. 8]. During strong backflow, time evolution diminishes P_b until it becomes commensurate with values expected from random superpositions; however, there is a quantum revival at $t = 2\pi$ due to the periodicity of ψ.

4. What backflows?

The aim of this section is to investigate which systems can exhibit backflow. So far we have only looked at the very simple case of superpositions of plane waves, where the wavefunctions are assumed to represent non-relativistic spinless particles governed by the Schrödinger equation. Of course, quantum mechanics describes a vast array of particles with varying properties and it is plausible that some, if not many, of these can exhibit the backflow effect. Equally possible is backflow of an entirely different kind, no longer related to the direction of the particle's linear momentum. It has been stressed that backflow originates in the non-commutativity of position and momentum; which other uncertainty relations provide a source for the effect? It is these kind of questions which we hope to explore and answer in this section.

4.1 Backflow in opposition to a force

In Bracken and Melloy's first paper [4] and, indeed, Allcock's original paper on the topic [3] only a free non-relativistic Schrödinger particle is considered. In their third paper on the problem [8], Bracken and Melloy consider the case of a non-relativistic particle moving under a constant force. Remarkably, they discover that, in this case, backflow can still occur in direct opposition to the force.

Consider a spinless particle moving non-relativistically in 1-dimension under a constant force $F \geq 0$ in the positive x-direction with a wavefunction made up entirely of positive momentum plane waves. Its probability density and current are in the the usual

form given by Eqn.(2.1) and Eqn.(2.2) respectively. Although the particle is subject to a constant force and the momentum remains positive, the current $J(x,t)$ can still be negative. As with the free case we want to know what the amount maximum of probability that can flow backwards is.

The Hamiltonian for the system is,

$$H = \frac{p^2}{2m} - Fx \tag{4.1}$$

and the time evolution for the state has the usual form,

$$U(t) = e^{-itH/\hbar}\,. \tag{4.2}$$

We specify that our state in momentum-space, $\phi(p)$, vanishes for $p < 0$. In the position representation our wavefunction has the form,

$$\psi(x,t) = \frac{1}{\sqrt{2\pi\hbar}} \int_{Ft}^{\infty} e^{ixp/\hbar} e^{-i(p^2t - Ft^2p)/(2m\hbar)} \phi(p - Ft)\, \mathrm{d}p\,. \tag{4.3}$$

As with the free case in Section 2, we wish to set up an eigenvalue equation which allows us to find the most negative eigenvalue Λ. Here, Λ is the equivalent of c_{bm} for the free case and all eigenvalues of the backflow operator under a force lie in the range $-\Lambda \leq \lambda \leq 1$.

Our eigenvalue equation is given by,

$$\frac{1}{\pi} \int_0^{\infty} \frac{\sin[u^2 - v^2 + \alpha(u-v)]}{u - v} \varphi(v)\, \mathrm{d}v = \lambda \varphi(u) \tag{4.4}$$

where

$$\alpha = \frac{FT^{\frac{3}{2}}}{\sqrt{4m\hbar}} \tag{4.5}$$

is a dimensionless parameter. Note that we have made the same substitutions for p and q as in the free case ,Eqn.(2.14), which is recovered when $\alpha = 0$. Eqn.(4.4) was not solved analytically but Bracken and Melloy solved it numerically for various values of α ranging

from 0 to 1.25 and their results can be seen in Fig.(3) below. Attempts to fit these results to an equation suggest the following relation,

$$\Lambda = -0.039e^{-2\alpha} \approx -c_{bm}e^{-2\alpha}. \tag{4.6}$$

This equation closely fits the numerical results obtained by Bracken and Melloy which leads them to propose Eqn.(4.6) as an exact relation and that Eqn.(4.4) is analytically solvable.

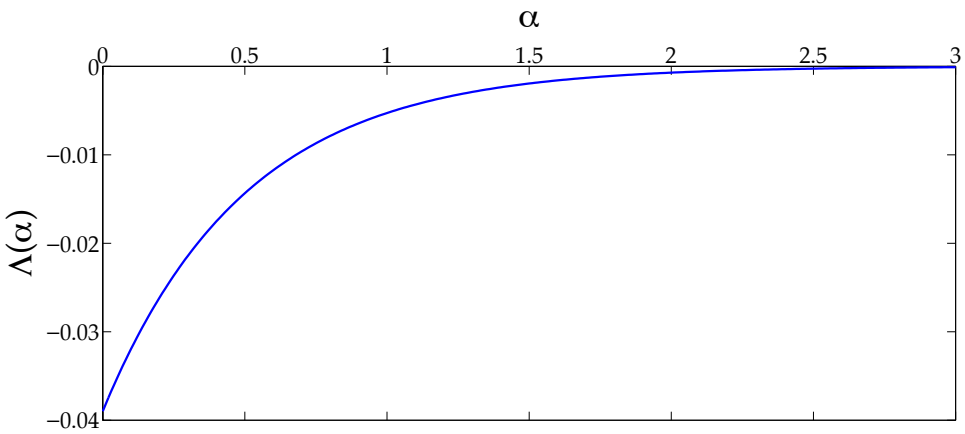

Figure 3: A plot of the most negative eigenvalue $\Lambda(\alpha)$ as a function of α.

Eqn.(4.6) invites some comment. In contrast to the free case, where remarkably c_{bm} is independent of all parameters in particular $\hbar$, we see that Λ is dependent on our new dimensionless parameter α which in turn is explicitly dependent on the force F, backflow duration T, particle mass m and $\hbar$. Note first that in the limit $F \to 0$ then Λ simply becomes c_{bm} because $\alpha = 0$. This is expected, we have recovered the free case by setting the force to 0. Also expected is that Λ decreases with increasing F and decreasing $\hbar$ (the näive classical limit). Surprisingly however, Λ increases with increasing m which is unexpected because large m would normally correspond to a classical scenario in which backflow surely ceases. The effect vanishes when $T \to \infty$ which represents the fact that although we can have periods of backflow, overall the particles direction of travel is positive.

4.2 The Dirac electron

We now consider the case of a relativistic Dirac particle and find that like the example above, where a force was introduced, the maximum amount of backflow becomes parameter dependent [9]. Non-relativistic behaviour must be a limiting case of the more general relativistic description, so we should expect that backflow occurs for a relativistic particle. If we were to find that backflow does not occur in the relativistic case then there must be good explanation, otherwise, it would indicate that backflow arrises from a failure of quantum mechanics to correctly describe non-relativistic behaviour.

Again we consider a particle moving in 1-dimension along the x-axis. The wavefunction for a Dirac particle has two complex-valued components,

$$\Psi(x,t) = \begin{pmatrix} \psi_1(x,t) \\ \psi_2(x,t) \end{pmatrix} . \tag{4.7}$$

The Hamiltonian for the system in terms of the particle's momentum p is,

$$H = c\sigma_1 p + \sigma_3 mc^2 \,, \tag{4.8}$$

where c is the speed of light and σ_i are the Pauli matrices. The wavefunction (4.7) obeys the Dirac equation,

$$i\hbar \frac{\partial \Psi(x,t)}{\partial t} = H\Psi(x,t) \,, \tag{4.9}$$

and its current is expressed as,

$$J = c\Psi^\dagger \sigma_1 \Psi = c[\psi_1^*(x,t)\psi_2(x,t) + \psi_2^*(x,t)\psi_1(x,t)] \,. \tag{4.10}$$

As with the previous cases we restrict our analysis to solutions consisting only of positive momentum components and we require the additional restriction to positive energy solutions.

We wish to find the maximal amount of probability that can flow backwards and how

this value depends on physical parameters. The analysis provided by Bracken and Melloy is identical in structure to the free case [4] and motion under a force [8] so we summarise here briefly. To find the maximum amount of probability backflow Λ at $x = 0$ during the interval $[0, T]$ we write the eigenvalue equation,

$$\frac{1}{\pi}\int_0^\infty \frac{\sin[2(\mathcal{E}(u)-\mathcal{E}(v))/\epsilon^2][u(\mathcal{E}(v)+1)+v(\mathcal{E}(u)+1)]}{[2(\mathcal{E}(u)-\mathcal{E}(v))/\epsilon^2]\sqrt{\mathcal{E}(u)[\mathcal{E}(u)+1]\mathcal{E}(v)[\mathcal{E}(v)+1]}}\phi(v)\,\mathrm{d}v = \lambda\phi(u) \tag{4.11}$$

where

$$\epsilon = \sqrt{\frac{4\hbar}{mc^2T}}\,, \tag{4.12}$$

$$\mathcal{E}(p) = \frac{\sqrt{p^2+m^2c^2}}{mc} \tag{4.13}$$

and the substitutions $p = umc\epsilon$ and $q = vmc\epsilon$ have been made [9].

In the non-relativistic limit where $c \to \infty$, then $\epsilon \to 0$ and $\mathcal{E}(u) \to 1 + \epsilon^2u^2/2$; we see that Eqn.(4.11) reduces to the simple free case Eqn.(2.15) from Bracken and Melloy's original paper [4]. Again no analytical solution was forthcoming so numerical methods were applied. Below is a plot of the results obtained for 4 values of ϵ in the range $[0.01, 1]$. Unlike the case of backflow in opposition to a force, Bracken and Melloy do not propose an exact relation between Λ and ϵ however it is clear from Fig.(4) that the relation is linear and Λ decrease monotonically with increasing ϵ. As we would expect Λ converges to $c_{bm} = 0.039$ in the non-relativistic limit; however its behaviour as other parameters change is somewhat unexpected. In particular, Λ obtains its extremal value 0.039 in the limits $m \to \infty$ or $\hbar \to 0$, both of which correspond to classical scenarios. This strange behaviour with increasing m was seen in the above case of motion under a force and certainly requires further investigation to understand its cause. The $\hbar$ dependent behaviour although equally counter-intuitive is less worrying, as we have already seen in the free case that backflow doesn't seem to disappear in the näive classical limit. How to restore this limit will be discussed at length in section 6. If we set $T \approx \hbar/mc^2$, which is a relativistic timescale of the order 10^{-21}, the backflow effect is greatly diminished indicating that

relativistic corrections to the effect would be almost impossible to detect experimentally.

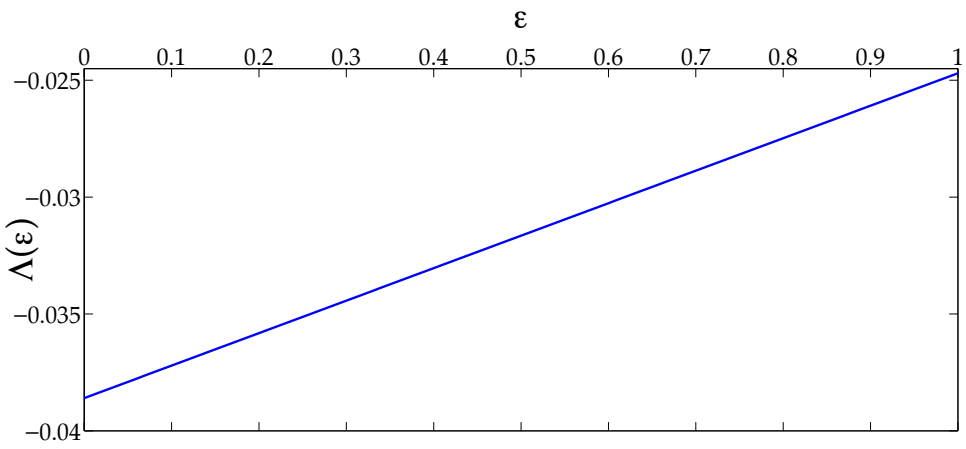

Figure 4: A plot of the most negative eigenvalue $\Lambda(\epsilon)$ as a function of ϵ.

The above two examples demonstrate that backflow is not limited to the case of a free non-relativistic particle but can in fact be (theoretically) observed in a variety of situations. We now move on to look at an entirely different kind of backflow in which the quantity that is being 'flowed back against' is no longer linear momentum.

4.3 Angular momentum backflow

It has been mentioned here and by various authors [7, 10] that backflow originates in the Heisenberg uncertainty relations. So far the only uncertainty relation that has been discussed here is that which obtains between position and linear momentum. It is therefore interesting to ask which other uncertainty relations can act as a 'source' of the effect. This is the line of thought Strange takes when deriving a new example of the backflow effect in action [10]. Uncertainty relations can be found between any two non-commuting observables and here we investigate the backflow properties of the angular momentum-azimuthal angle uncertainty relation.

The Schrödinger equation for an electron in a constant magnetic field $\vec{B}$ is well known and can be analytically solved [36]. We require only a few details from the calculation

for our purposes. In cylindrical polar coordinates (r, ϕ, z) our vector potential is, $\vec{A} = (0, \frac{1}{2}Br, 0)$. The form of the Schrödinger equation and eigenfunction solutions are somewhat complicated and we refer the reader to chapter 15 of [36] for details. The current can be written as,

$$\vec{J}(\vec{r}, t) = \frac{\hbar}{2im}[\psi^*(\vec{r}, t)\nabla\psi(\vec{r}, t) - \psi(\vec{r}, t)\nabla\psi^*(\vec{r}, t)] - \frac{e\vec{A}}{m}|\psi(\vec{r}, t)|^2 \tag{4.14}$$

$$= \vec{j}_1(\vec{r}, t) - \vec{j}_2(\vec{r}, t)\,. \tag{4.15}$$

The current has no radial components which can be verified by working out each term in Eqn.(4.15) [10]. The energy eigenvalues for solutions of the Schrödinger equation are,

$$E_{n,l} = (n + \tfrac{1}{2}|l| + \tfrac{1}{2}l + \tfrac{1}{2})\hbar\omega\,, \tag{4.16}$$

where n is a non-negative quantum number required to make the eigenfunctions finite, l is a quantum number associated to the electron's angular momentum and $\omega = eB/m$ [10]. We define our wavefunction as a linear combination of the eigenstate solutions with fixed n, non-positive l and no motion in the z-direction,

$$\psi(\vec{r}) = \sum_{l=l_{\text{min}}}^{L} a_l(\vec{r})e^{il\phi}\,, \tag{4.17}$$

where a_l are real coefficients containing the radial dependence and orthogonality of the eigenstates and $L = l_{\text{max}}$[4]. It would be natural to think that this wavefunction can only have effective values of l which are negative as we imposed this condition on the individual eigenfunctions. However by rewriting Eqn.(4.17) in the amplitude-phase form we see that this is not the case,

$$\psi(\vec{r}, t) = \alpha(r, z)\text{exp}\left[i\int_0^{\phi} l(\phi')\,\mathrm{d}\phi'\right]\,, \tag{4.18}$$

[4]The value of l_{max} depends on how many eigenfunctions we want in our superposition (4.17)

where $\alpha(r,z)$ is the amplitude, ϕ is in the range $[0,2\pi)$ and the effective l quantum number is given by,

$$l^{\text{eff}}(\phi) = \frac{\partial}{\partial\phi}\arg\psi_(\vec{r}) = \frac{\vec{j}_1(r,t)}{\rho(r,t)}\,. \tag{4.19}$$

The probability density $\rho(\vec{r},t)$ cannot be negative which ensures that locally the angular momentum is always in the same direction as the current. Notice the almost identical structure of this analysis to that of Berry [23] given in section 3.3. This confirms the point made before, that by simply choosing another quantum mechanical uncertainty relation it is possible to derive a new backflow effect.

What is the angular momentum-azimuthal angle uncertainty relation? It is simply,

$$\Delta\phi\Delta\mathcal{L} \geq \hbar\,, \tag{4.20}$$

where $\mathcal{L}$ is the electron's angular momentum. An interesting feature of the above analysis is that this uncertainty relation (4.20) is implicit in the ϕ dependence of l^{eff} in Eqn.(4.19). So although Eqn.(4.20) is a well known relation, "determinig the backflow quantitatively demonstrates the subtle structure that underlies the quantum mechanical uncertainty in this system" [10, p. 5].

Strange proceeds to illustrate the backflow effect with 3 versions of the wavefunction (4.17) : a 3-eigenfunction superposition which can be solved analytically, a 2-eigenfunction superposition and an 11-eigenfunction superposition which must be computed numerically. For the 3-eigenfunction case there are substantial regions of backflow. A crucial difference between this angular momentum backflow and the linear momentum backflow studied above is that in this case the effect can last indefinitely. Pervious authors [4, 7–9, 23] considered wavefunctions in which the different time dependence of the component waves caused the backflow regions to decay. Here the system's energy is independent of the l quantum number so the time dependence of all eigenstates is identical which results in a backflow effect that lasts indefinitely.

4.4 Summary

The focus of this section has been on what types of physical systems can demonstrate backflow and has revealed that the range is potentially limitless. The work of Bracken and Melloy [8, 9] dispels the notion that backflow is an artefact of idealised quantum mechanics and opens up the possibility of studying backflow in highly realistic systems undergoing forces and relativistic motion. These systems with greater complexity introduced parameter dependence to the backflow so rather than the amount of probability flowing back being arbitrary it now depends on the physical features of the system. This dependence is expected and its absence in the original free case [4] was perplexing, suggesting that realistic models of backflow may provide clues to experimentation.

Strange [10] addressed a different concept. Rather than investigate what variations or additions can be made to the free backflow system of section 2, he considered an entirely new type of backflow. His work is fascinating because with exactly the same analysis as Berry [23] he revealed an entirely different effect: backflow of angular rather than linear momentum. An obvious course of investigation is to check what other types of backflow exist; the possibilities are great considering the unlimited number of uncertainty relations. An intriguing prospect is negative energy backflow originating in the time-energy uncertainty relation. A related question is to ask which states within the systems considered (in particular the free case) can exhibit backflow; not all states can and it is revealing to determine those that do. It is to this that we turn in the next chapter.

5. Backflow states

In this section we will discuss the variety of states that can give rise to the backflow effect. Of course not every quantum state does realise backflow and it is important to understand what the features of and the differences between those that do are. Various states have been proposed in the literature [4, 7–11, 20, 23] many of which are similar in structure; some are merely demonstrative examples with no physical realisation while others have the potential to be experimentally verified. The aim of this section is to clarify all these issues.

5.1 The Wigner function

Is there a way of knowing whether a particular state can exhibit backflow? One clue may lie in the Wigner function,

$$W(x,p,t) = \frac{m}{2\pi\hbar}\int_{-\infty}^{\infty} e^{-ipy/\hbar}\psi^*(x-\tfrac{1}{2}y,t)\psi(x+\tfrac{1}{2}y,t)\,\mathrm{d}y\,. \tag{5.1}$$

It is the closest quantum mechanical analogue to the classical probability distribution function. This has led some to suggest it be used as an arrival time distribution [14]. We can write the probability of a particle with positive momentum located in $x<0$ arriving at $x=0$ during the interval $[t_1,t_2]$ as the difference between the probabilities of being located in $x<0$ before and after this period, i.e. the flux, Eqn.(2.5), over this time interval. This

can be rewritten in terms of the Wigner function,

$$F(t_1, t_2) = \int_{t_1}^{t_2} \mathrm{d}t \int \frac{p}{m} W(-pt/m, p, 0)\mathrm{d}p\,, \tag{5.2}$$

where $W(x, p, t) = W(x - pt/m, p, 0)$ for a free particle. Simply replacing W with its classical analogue the probability distribution function ω would yield the classical arrival time distribution. However the Wigner function is not generally positive even for positive momentum states and concern over the interpretaion of negative probabilities has led to a rejection of the Wigner function as an equivalent replacement for the classical distribution.

However note that Eqn.(5.2) implies that we can rewrite the current as,

$$J(x, t) = \int_0^\infty \frac{p}{m} W(x, p, t)\mathrm{d}p\,. \tag{5.3}$$

That the Wigner function can be negative indicates that both J and F can also be negative for some states. In fact negativity of the Wigner function is a necessary condition for negative flux [17]. Unfortunately it is not a sufficient condition, since a negative Wigner function can still result in a positive flux via Eqn.(5.2) [7]. All backflow states, therefore, must have negative Wigner functions but this in itself does not tell us whether a state will exhibit backflow. We shall therefore investigate a variety of functions that do in order to understand their features.

5.2 Plane waves

We start the study with the simplest of cases: a superposition of two planes waves. This state, used by Bracken and Melloy in the original paper [4], is easy to work with and ably demonstrates the possibility of backflow. It is however non-normalisable which by definition makes it unphysical.

Here and for the rest of this chapter we work in units where $\hbar = m = 1$. Our wave-

function has the simple form,

$$\psi(x,t) = \sum_{n=1,2} A_n e^{ip_n(x-p_n t)} \,. \tag{5.4}$$

The current at $x = 0$ is given by Eqn.(2.2) and is,

$$J(0,t) = A_1^2 p_1 + A_2^2 p_2 + A_1 A_2 (p_1 + p_2) \cos[(p_1 - p_2)t] \,, \tag{5.5}$$

which oscillates between a maximum value of $(A_1 p_1 + A_2 p_2)(A_1 + A_2)$ and a minimum value of $(A_1 p_1 - A_2 p_2)(A_1 - A_2)$. If we set the parameters such that $A_1 > A_2$ and $A_1 p_1 < A_2 p_2$ then the current is negative and the state undergoes backflow.

We saw in section 3 that Berry used various plane-wave superpositions throughout his work [23] which were generalisations of Eqn.(5.4). Simple wavefunctions like Eqn.(3.30) are easy to work with and convenient for demonstrating results however they are not normalised and therefore unphysical. In addition to the above plane wave (5.4), Bracken and Melloy provided examples of normalised wavefunctions; we saw one of these, Eqn.(4.3), when discussing motion under a force. We now look at an equivalent example for the free case.

Our wavefunction has the form,

$$\psi(x,t) = \frac{1}{\sqrt{2\pi}} \int_0^\infty e^{ixp} e^{-ip^2 t/2n} \phi(p) \mathrm{d}p \,, \tag{5.6}$$

with,

$$\phi(p) = \frac{18}{\sqrt{35\xi}} p \left[e^{-p/\xi} - \tfrac{1}{6} e^{-p/2\xi} \right] \quad p > 0 \tag{5.7}$$

where ξ is a positive constant with dimensions of momentum and $\phi(p) = 0$ for $p < 0$. The current, Eqn.(2.2), for this wavefunction is,

$$J(x,t) = \frac{1}{4\pi} \int_0^\infty \int_0^\infty e^{ix(p-q)} e^{-it(p^2-q^2)/2m} \phi(p) \phi^*(q) \mathrm{d}p \, \mathrm{d}q \,. \tag{5.8}$$

We can calculate the value of the current at the origin at $t = 0$,

$$J(0,0) = -\frac{36\xi^2}{25\pi}\,, \tag{5.9}$$

which is clearly negative. So the wavefunction immediately exhibits backflow from its initial state; Bracken and Melloy calculate that this continues until $t_1 \approx 0.021/\xi^2$. The flux during this interval is $F = -0.0043$ which is approximately 11% of the theoretical maximum, c_{bm}. This is a small but not insignificant amount of probability backflow and demonstration of this effect with a normalisable wavefunction is an important achievement. When investigating backflow for a relativistic Dirac particle [9], Bracken and Melloy use an identical wavefunction to Eqn.(5.6) however the form of Eqn.(5.7) is different, taking account of the relativistic and spinor nature of the particle.

5.3 Gaussian wavepackets

We saw in the section above that certain superpositions of plane waves could easily demonstrate the backflow effect; their drawback was that, in most cases, they are unrealistic. Here we will look at a superposition of Gaussians which has two benefits: firstly they are physical and realistic which shows that backflow is not purely theoretical and secondly they are experimentally realisable wavefunctions. Experimental verification of backflow will be discussed in section 7 but for now we note that it is feasible to produce Gaussian wavepackets in the lab. Unfortunately, Gaussians have support on both positive *and* negative momentum, so it will be necessary to show that the negative current doesn't originate from the negative momentum of the state.

We begin with the superposition of two Gaussian wavepackets,

$$\psi(x,t) = \sum_{n=1,2} A_n \frac{1}{\sqrt{4\sigma^2 + 2it}} \exp\left[ip_n(x-p_n) - \frac{(x-p_nt)^2}{4\sigma^2+2it}\right]\,. \tag{5.10}$$

This is a normalised state where σ is the spatial width of the Gaussians. Note that as

$\sigma \to \infty$ the state tends to Eqn.(5.4), our initial plane wave superposition. Yearsley et al suggest that this indicates that if σ is large enough then the current $J(x,t)$ of our gaussian superposition will be the product of Eqn.(5.5) and some slowly varying function [7] . We would then expect backflow to be present in the Gaussian case too. The expression for this current is complicated and is not given by Yearsley et al however they provide a number of plots which beautifully illustrate the backflow effect, two of which are shown below (see Fig.(5) and Fig.(6)).

The following parameters were found by Yearsley et al [7] to produce the greatest amount of backflow[5],

$$p_1 = 0.3, \quad p_2 = 1.4, \quad \sigma = 10, \quad A_1 = 1.8, \quad A_2 = 1. \tag{5.11}$$

Using these values, plots for the time dependence of the current at $x = 0$ and the probability of remaining in the half-space $x < 0$ were obtained. Fig.(5) and Fig.(6) both show that backflow can occur at multiple disjoint intervals. In order to calculate the maximum amount of probability backflow we must choose the maximal interval, $[t_1, t_2]$, during which the current is negative the entire time. Using Eqn.(2.6) the flux is calculated to be $F \approx -0.0061$. This is approximately 16% of the theoretical maximum c_{bm}.

However, as we mentioned above, there is the possibility that the negative current shown at $x = 0$ actually originates from the negative momentum support of the Gaussians. In order to confirm that our above example demonstrates backflow we must show that this is highly improbable. Our two Gaussians are centred around different momenta so we focus on the one around $p = 0.3$. The probability that the momentum of this state is measured to be negative is approximately given by [7],

$$P(p < 0) \sim \int_{-\infty}^{0} e^{-200(p-0.3)^2} \mathrm{d}p \sim 10^{-10} \,. \tag{5.12}$$

[5]These values were found by searching the parameter space of states exhibiting backflow. However by their own admission the search was far from exhaustive, thus it remains possible that a different set of parameters will produce greater backflow.

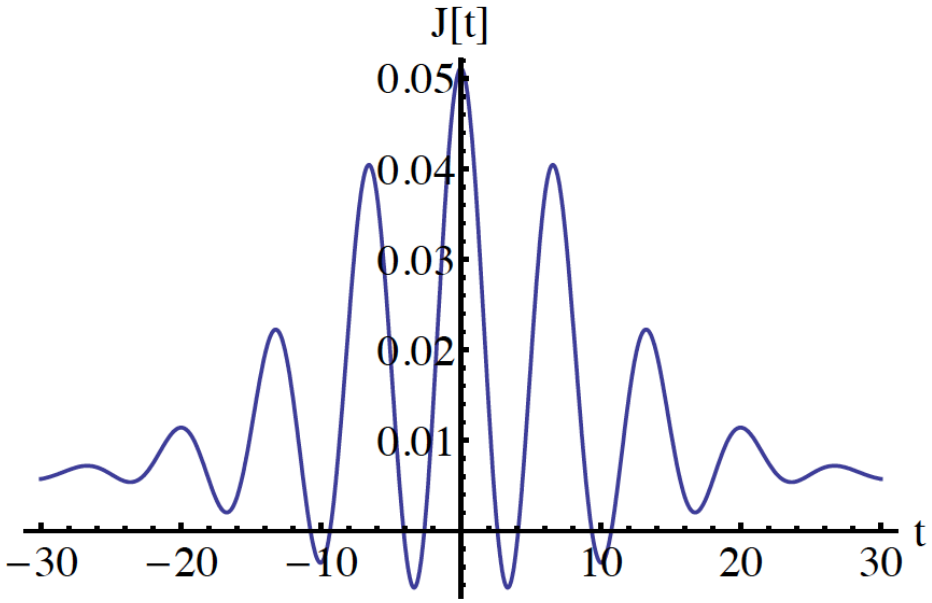

Figure 5: Plot of the current for a superposition of two Gaussians with parameters given by (5.11) [7].

$P(p < 0)$ is clearly so small as to be negligible and we can assume the negative current is entirely due to backflow. The backflow from our superposition of Gaussians is greater than that obtained from our superposition of plane waves (5.6) which suggests that as well as being more realistic, Gaussians may also be better at producing large backflow. Muga et al [16] used a single Gaussian in momentum space when discussing the relation between perfect absorbers and backflow. However they note that their function is non-trivial due to the restriction of no negative momentum components. The eigenfunctions used by Strange [10] and discussed in section 4.3 were also very complicated Gaussians and somewhat difficult to work with. Such difficulties emphasise the significance of Yearsley's result using only a superposition of two simple Gaussians.

5.4 An exhaustive class

In a very recent paper [22] Halliwell et al have discovered a broad class of states for which it is always possible to set the parameters such that there is backflow. By writing the

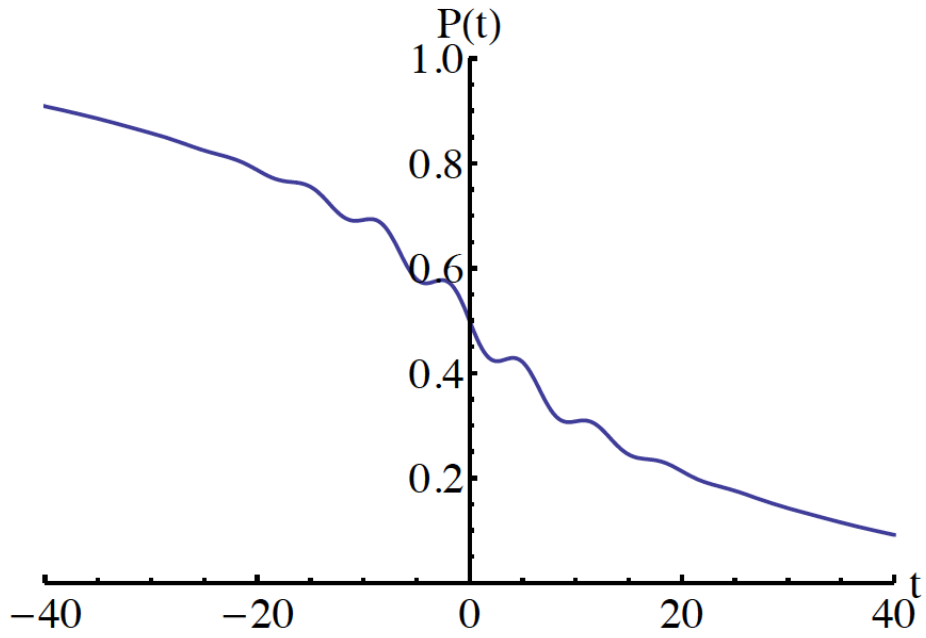

Figure 6: Plot of the probability of staying in $x < 0$ for a superposition of two Gaussians with parameters given by (5.11) [7].

current Eqn.(2.2) in momentum space one can derive a simple inequality for generating a negative current. Solutions to this inequality are best written in the form,

$$\phi(p) = N\theta(p)(a-p)f(p)\,, \tag{5.13}$$

where N is a real normalisation factor, a is complex and $f(p)$ is a normalised complex state function. Subject to the correct conditions[6], any function can be written in this form (in particular Eveson et al).Remarkably, Halliwell et al were able to show that as long as the current exists and doesn't vanish there is always a value which a can take to produce backflow. A simple example is to set $f(p)$ as a Gaussian so that Eqn.(5.13) reads,

$$\phi(p) = N(a-p)e^{-\gamma_0^2 p^2} \tag{5.14}$$

[6]We refer the reader to the original paper [22].

where a and γ_0 are real constants to be determined and N is given by,

$$N^2 = 2\gamma_0\sqrt{\frac{2}{\pi}}\left(a^2 + \frac{1}{4\gamma_0^2} - \frac{a}{\gamma_0}\sqrt{\frac{2}{\pi}}\right)^{-1} \tag{5.15}$$

The current for this state can be calculated analytically at any time — which is an advantage over some of the other examples — and primarily depends on the dimensionless quantity $a\gamma_0$. A plot of the current is reproduced below in Fig.(7) for the state with the most negative flux, produced by setting $a\gamma_0 = 0.684$. There is emphatic backflow around $t = 0$ but only briefly, as we see that the current rapidly changes from positive to negative and back again. The backflow flux was numerically computed for this state and found to be $F(t_1, t_2) \approx -0.01573$ which is approximately 41% of the theoretical maximum c_{bm} [22]. The authors note that this state is relatively easy to produce experimentally and therefore could be useful in verifying the effect.

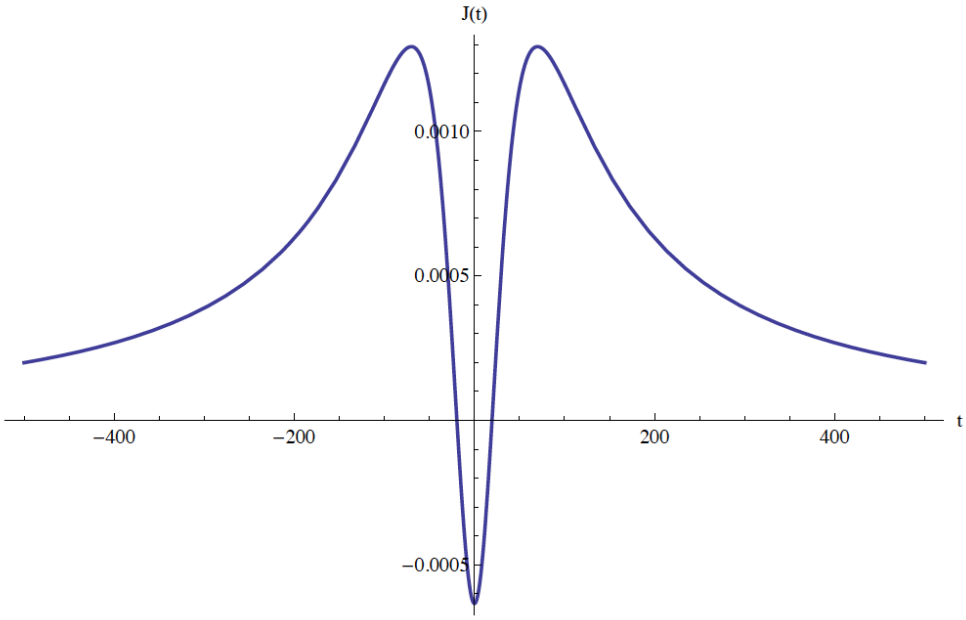

Figure 7: The current $J(t)$ for the state (5.14) [22].

5.5 Maximising backflow

In addition to rigorously defining the backflow operator and improving the accuracy of Bracken and Melloy's bound c_{bm}, Penz et al [6] attempted to find a backflow maximising state. This can be achieved by finding solutions to Eqn.(2.15). Unable to do so analytically, Penz et al numerically found an approximate eigenstate of Eqn.(2.15) for which the eigenvalue was $-c_{bm}$. Fig.(8) plots the state's current with a clear period of backflow when $-1 < t < 1$. Note the unusual singularity behaviour at $t = \pm 1$, likely a feature of the flux operator. Is it possible to find an analytic expression which is an eigenstate of Eqn.(2.15) with $-c_{bm}$ as its eigenstate? Presently no one has achieved this aim but Yearlsey et al have made significant headway and found expressions which achieve high levels of backflow [7].

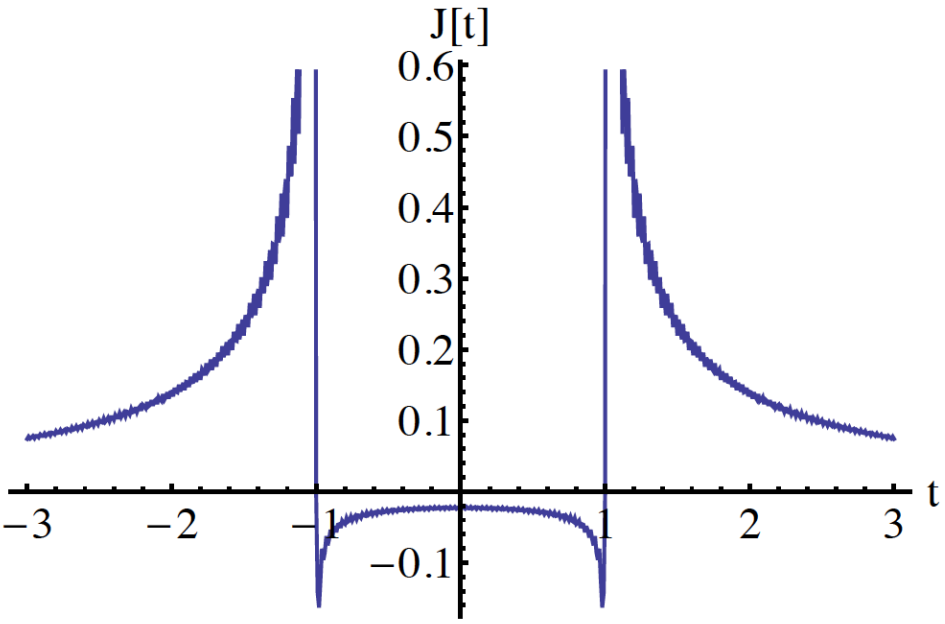

Figure 8: A plot of the current for the backlfow maximising state [21].

Based on the work of Penz et al, Yearlsey et al guess functions which approximate the behaviour of the maximal state (see Fig.(8)) and check that they have negative current.

The numerically computed maximal backflow state has the asymptotic form,

$$\phi_{\text{asy}}(u) = a\frac{\sin u^2}{u} + b\frac{\cos u^2}{u}\,. \tag{5.16}$$

Yearsley et al find that this fits the maximal state best when $a = 0$ and $b = -0.1$. It was not difficult to find states that approximately match this behaviour and have negative current however it was extremely difficult to match the singularity structure at $t = \pm 1$ and we repeat here their best attempt to do this.

The momentum space wavefunction is,

$$\varphi(u) = N\left[ae^{-bu} + [\tfrac{1}{2} - C(u)]\right]\,, \quad a, b \in \mathbb{R}\,, \tag{5.17}$$

where C is the cosine Fresnel integral,

$$C(u) = \int_0^x \cos(x^2)\,\mathrm{d}x \tag{5.18}$$

and N is a normalisation factor given by,

$$N^{-2} = \int_0^\infty \left(a^2e^{-2bu} + [\tfrac{1}{2} - c(u)]^2 + 2ae^{-bu}[\tfrac{1}{2} - c(u)]\right)\mathrm{d}u\,. \tag{5.19}$$

Eqn.(5.17) has the asymptotic form,

$$\varphi(u) \sim N\frac{\sin u^2}{u}\,, \tag{5.20}$$

which shows good agreement with the numerical results of Penz et al. Because Eqn.(5.17) is only an approximate eigenstate of the flux operator, the backflow interval when $J(t)$ is negative won't exactly coincide with the range $[-1, 1]$. Instead we use the interval $[t_1, t_2]$ in Eqn.(2.6) and adjust this range to fit the backflow region. The process of computing the current and then the flux is somewhat complicated and we refer the reader to the original

paper [7] for details. With $a = 0.6$ and $b = 2.8$ the maximum amount of flux over this range is,

$$F = -0.02757\,, \tag{5.21}$$

which is approximately 72% of the theoretical maximum, c_{bm}. This is a very impressive result, however the fact that the state doesn't have the maximal amount of negative flux indicates that its behaviour won't fully match the numerical maximal state. A plot of the current as a function of time reveals this to be the case. Fig.(9) shows that although our function (5.17) matches the general behaviour of the maximum state it is noticeably different as $t \to \pm 1$ when compared to Fig.(8). Fig.(10) is of the probability of staying in the half space $x < 0$ and emphatically shows the probability increasing in the range $-1 < t < 1$. Note also the rapid decrease in probability near $t = \pm 1$ which corresponds to the singularity behaviour of the current at those times. It is clear that the structure of the wavefunction at $t = \pm 1$ is crucial to finding an exact solution to Eqn.(2.15) and it is likely that when this is achieved it will bring greater understanding to the nature of backflow.

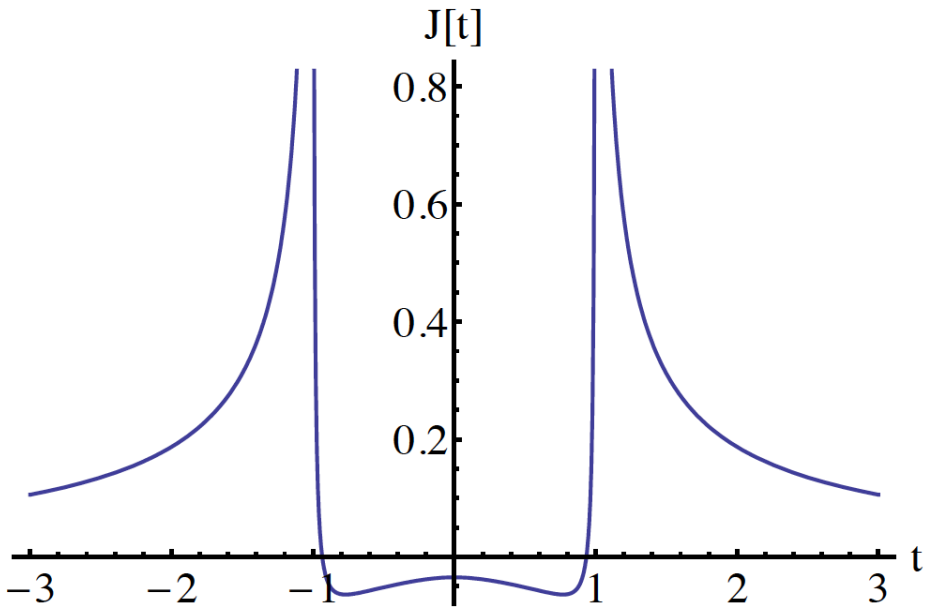

Figure 9: A plot of the current for the guessed state (5.17) with $a = 0.6$ and $b = 2.8$ [7].

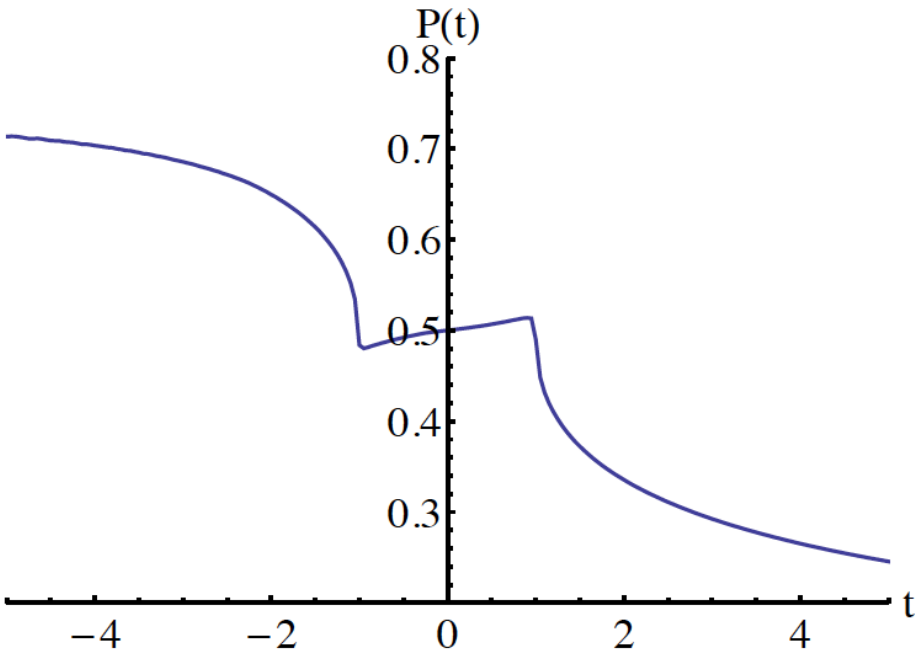

Figure 10: A plot of the probability of staying in $x < 0$ for the guessed state (5.17) with $a = 0.6$ and $b = 2.8$ [7]. It is a striking illustration of the backflow effect.

6. The classical limit

Backflow is a quantum mechanical effect unseen in any classical experiment. It is to be expected therefore, that as one introduces a classical limit to a backflow system, the effects should disappear. However we saw in previous sections that there is no obvious way to do this in the case of the free particle. The probability backflow limit, c_{bm}, is a dimensionless constant independent of any physical parameters and how backflow changes with scale is unclear. Simply letting $\hbar \to 0$ does nothing as their is no obvious $\hbar$ dependence in the backflow effect. In contrast to the free case both backflow in opposition to a force [8] and backflow of a relativistic Dirac particle [9] were dependent on physical parameters. Upon introducing a force we found the relation $\Lambda \approx -c_{bm}e^{-2\alpha}$ where α is a dimensionless parameter dependent on the physical features of the system. Likewise, for a relativistic Dirac particle we found that the amount of backflow depended on ϵ, another dimensionless parameter which was also a function of the system's attributes. However the parameter dependence was not all as one would expect (or like); in particular backflow actually increased in the relativistic case as $\hbar \to 0$ contrary to expectations. Yet the inclusion of parameters suggests possibilities for restoring the classical limit. In particular one could argue that relativistic motion and motion under a force are more realistic descriptions of a quantum system than an entirely free non-relativistic particle. That these descriptions resulted in parameter dependence suggests that if we attempt to describe a more realistic model for our backflow system our classical limit may be restored.

A common method of investigating the classical limit of quantum systems, or more precisely how classicality emerges, is to describe the system as coupled to large environ-

ment and then study the evolution of the reduced density matrix for the particle. In a model of this type the Wigner function will become positive after a brief period of time [37]; we have already seen that negativity of the Wigner function is a necessary condition for backflow. Yearsley has investigated the relation between the Wigner function, current and the environment in a work focused on arrival times [17] and shown that after a finite time the current always becomes positive. The focus here will instead be on reintroducing $\hbar$ dependence through the use of a more realistic model for backflow, in particular by redefining the flux operator.

In section 2 our flux operator, Eqn.(2.9), was defined in terms of the projection operator $\hat{P} = \theta(\hat{x})$; instead we will now define it in terms of a quasi-projector $\hat{Q}$. Any measurements performed in a backflow experiment would necessarily be imprecise and are best modelled by quasi-projectors so this is an acceptable substitution [7]. We define our quasi-projector as,

$$\hat{Q} = \int_0^\infty \delta_\sigma(\hat{x} - y)\mathrm{d}y \tag{6.1}$$

where $\delta_\sigma(\hat{x} - y)$ is a smoothed δ-function,

$$\delta_\sigma(\hat{x} - y) = \frac{1}{\sqrt{2\pi\sigma^2}} e^{-(\hat{x}-y)^2/2\sigma^2} \tag{6.2}$$

which becomes the normal δ-function as $\sigma \to 0$. In this limit, $\hat{Q} \to \hat{P}$. Substituting $\hat{Q}$ for $\hat{P}$ in Eqn.(2.11) gives our new definition of the flux which can be expressed in terms of the redefined current operator,

$$\hat{J} = \frac{1}{2m}[\hat{p}\delta_\sigma(\hat{x}) + \delta_\sigma(\hat{x})\hat{p}] \tag{6.3}$$

In rough terms, the commutator of $\hat{p}$ and $\delta_\sigma(\hat{x})$ gets smaller as σ gets larger which results in a less negative flux. We can already see that the simple substitution of quasi-projectors for strict projectors could lead to a suppression of the bacfklow effect.

Our eigenvalue equation (2.15) becomes,

$$\frac{1}{\pi}\int_0^\infty \frac{\sin(u^2-v^2)}{u-v} e^{-a^2(u-v)^2}\varphi(v)\,\mathrm{d}v = \lambda\varphi(u), \tag{6.4}$$

where a is a dimensionless number given by $a^2 = 2m\sigma^2/\hbar T$. Our eigenvalues are parameter dependent through a because now $\lambda = \lambda(a)$. Crucially λ now depends on $\hbar$ and the limit $\hbar \to 0$ corresponds to $a \gg 1$ where $\hbar \ll 2m\sigma^2/T$. We expect that as a increases so will the eigenvalues λ so that they take their most negative value, $-c_{bm}$, only in the limit $a \to 0$. Hence the eigenvalues must satisfy the relation, $\lambda(a) \geq -c_{bm}$. To get a true sense of how λ depends on a it is necessary to compute some actual results and Yearsley et al calculated numerical estimates for $\lambda(a)$ while varying a [7]. A plot of these results is repeated below in Fig.(11). It is clear that $\lambda(a)$ does increase with a and tends to 0 asymptotically. Yearsley et al postulate that the relation may be of the form,

$$\lambda(a) \sim -\frac{1}{a^2} \tag{6.5}$$

for large a, which is suggested by the scaling behaviour of Eqn.(6.4) [7].

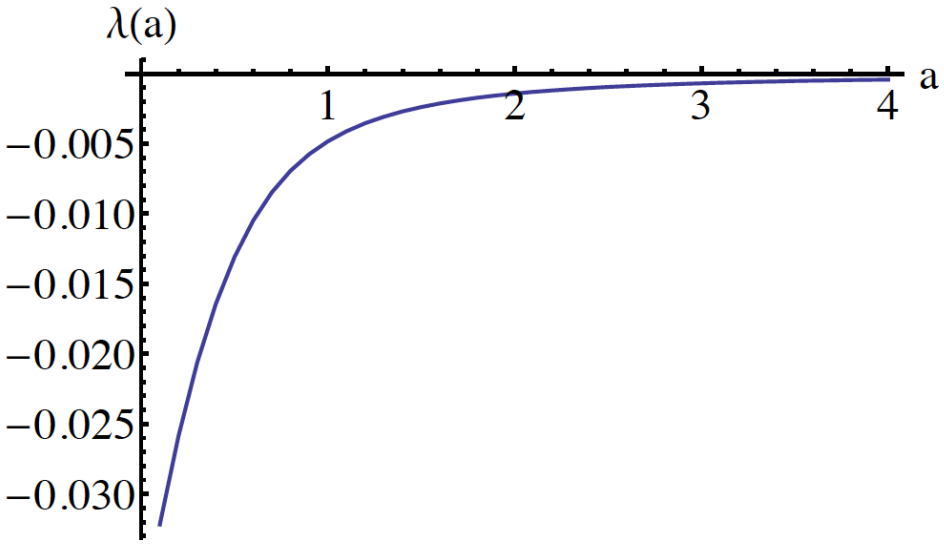

Figure 11: A plot of $\lambda(a)$ from (6.4) as a function of a [7].

It is crucial to check the behaviour of the positive eigenvalues; were these to tend to 0 as a increases then the analysis would be incorrect. Clearly positive current is a feature entirely consistent with a classical system and should remain unaffected as we reach the classical domain. Yearsley's numerical work confirms that eigenvalues in the range $[0, 1]$ (the positive part of the spectrum) remain largely unchanged when varying a so we can assume that the quasi-projector model is a sound method of introducing classicality.

It is clear that in order to introduce a classical limit to the backflow effect that a realistic model of the system is required. We have shown in detail how the use of quasi-projectors is one way to do this but other methods exist, often connected with the arrival-time problem [15]. Backflow is not unique in requiring a realistic description to restore the classical limit [7] and there is nothing surprising about an idealised system lacking all the relevant physical features.

7. Detecting backflow

Time in quantum mechanics has been considered a contentious concept since Allcock's trilogy of works [1–3] laid out the difficulties of both considering time as an observable and performing experiments which measure some type of time value. Allcock attempted to prove that one could not directly measure the arrival-time of a free particle to any accuracy; this has since been proved false [12] but the issues first raised by Allcock (including backflow) remain largely unresolved and open to differing opinions. One need only look at reviews of the field to see a broad range of open problems and interpretations of time related concepts [14, 15]. Much work has focused on the time of arrival for a particle, in particular whether there exists any operator that actually corresponds to such a measurement and the difficulties of an arrival-time experiment. Aharanov et al [12] argued that a time of arrival operator $\hat{T}_A$ cannot be precisely defined nor measured to arbitrary accuracy. They proved the relation $\Delta t_A \sim 1/E_k$ where Δt_A is the uncertainty in the measured time value, E_k is the particle's initial kinetic energy and here and throughout this chapter we use units in which $\hbar = 1$. This limit on the experimental accuracy is, unlike the uncertainty principle, dynamic rather than kinematic and arises due to the continuous interact between the measuring device and the particle. The relevance to our study is that classically one could consider the flux Eqn.(2.6) as the arrival-time probability distribution. Backflow suggests that this might not be the case quantum mechanically, as a negative flux would imply a negative probability for arriving at a point — a suggestion abhorrent to many physicists. Using the Decoherent Histories approach it has been shown that states for which there is decoherence have an arrival time distribution which coincides with the

flux [13, 38], a semiclassical result. However backflow states are precisely the kind for which there is no decoherence and this interpretation of the flux is not available [38].

The difficulties involved with time may be one of the reasons why an experimental verification of backflow is yet to be sought. Though backflow has been recognised for at least 20 years no one has attempted to measure backflow and test which states can exhibit the effect. Indeed until this year[7] no suggestion of an experimental set-up had even been made. The aim of this section is to discuss the issues surrounding a backflow experiment by investigating detector models and, in light of the just mentioned recent paper [20], feasible experimental set-ups.

7.1 Identical ensemble measurement

We saw in section 2 that the flux Eqn.(2.5) can be considered as the difference between two probabilities, therefore measuring these probabilities would essentially be a direct measurement of the flux [4, 7]. In order to do this one would need to prepare two identical ensembles of particles in the initial state $|\psi\rangle$. On the first ensemble one would measure each particle at $t = t_1$ to check if it is in $x < 0$ which would determine our probability $\langle P(t_1)\rangle$. These measurements would be repeated on the second ensemble at $t = t_2$ and hence ascertain $\langle P(t_2)\rangle$. If $\langle P(t_1)\rangle > \langle P(t_2)\rangle$ then the flux would be negative and the state has undergone backflow. If this seems surprisingly simple, that is because we have skimmed the details. There are difficulties involved in preparing large ensembles of identical states and as we mentioned in section 5 some backflow states would be difficult to create in the lab. There is also the added complication of 'measuring' a probability. As is clear from the above description this is not a one-shot measurement; probabilities by their very nature require many measurements to compute. The types of states we discussed which seemed experimentally viable produced no where near the maximum amount of backflow and would therefore require extremely accurate probability measurements in order to verify if the flux is negative. The combination of these factors makes this type

[7] 2013

of experiment extremely unlikely however they do not rule out the possibility of direct measurement by other means as we shall see below.

7.2 Detector models

We saw above that the arrival-time probability coincides with the flux in an appropriate semiclassical limit but that this does not occur precisely for states which exhibit backflow. It may then be informative to study arrival-time detection models and compare the positive semi-definite arrival-time probability with the possibly negative flux. This may give us hints as to the origin of negativity and possibly a method for detection. Most detailed and realistic measurement models use a complex potential and there are various examples of this in the literature [1–3, 7, 13, 14, 39]. The arrival-time probability distribution in such models is strongly linked with the current and may allow us to detect the signature of a negative current in the non-negative arrival-time distribution.

The model consists of a positive momentum wavepacket starting in $x < 0$ and a complex potential step function which acts as an absorber in $x > 0$. Our Hamiltonian is,

$$H = H_0 - iV_0\theta(\hat{x})\,, \tag{7.1}$$

where H_0 is the free Hamiltonian. Our initial state is evolved under the complex Hamiltonian,

$$|\psi\rangle = e^{-(iH_0+V_0\theta)\tau}\,|\psi_0\rangle\ , \tag{7.2}$$

the norm of which is the 'survival probability' at time τ,

$$N(\tau) = \langle\psi|\psi\rangle \tag{7.3}$$

$$= \langle\psi_0|e^{(iH_0-V_0\theta(\hat{x})|)\tau}e^{(-iH_0-V_0\theta(\hat{x})|)\tau}|\psi_0\rangle \tag{7.4}$$

We want to know the arrival-time probability distribution, $\Pi(\tau)\mathrm{d}\tau$, for crossing the origin

between τ and $\tau + \mathrm{d}\tau$; this is given by,

$$\Pi(\tau) = -\frac{\mathrm{d}N(\tau)}{\mathrm{d}\tau} = 2V_0 \langle\psi_0|e^{(iH_0 - V_0\theta(\hat{x})|)\tau}\theta(\hat{x})e^{(-iH_0 - V_0\theta(\hat{x})|)\tau}|\psi_0\rangle \tag{7.5}$$

However this expression doesn't explicitly show the current dependence which is ultimately what we want in order to understand its behaviour in the presence of backflow. If we differentiate with respect to τ we get,

$$\frac{\mathrm{d}\Pi}{\mathrm{d}\tau} = -2V_0\Pi + 2V_0 \langle\psi|\hat{J}|\psi\rangle \tag{7.6}$$

where $\hat{J}$ is the current operator Eqn.(2.8) introduced in section 2. This is solved to give,

$$\Pi(\tau) = 2V_0 \int_{-\infty}^{\tau} e^{2V_0(t-\tau)} \langle\psi_0|e^{(iH_0 - V_0\theta(\hat{x})|)t}\hat{J}e^{(-iH_0 - V_0\theta(\hat{x})|)t}|\psi_0\rangle \tag{7.7}$$

where we make the assumption that $\Pi(\tau) \to 0$ as $\tau \to -\infty$. We can now see the explicit current dependence of the arrival-time distribution in (7.7) which is positive by construction even though $\hat{J}$ might not be. Using this we can write an expression for the probability of crossing the origin during the interval $[t_1, t_2]$,

$$P(t_1, t_2) = \int_{t_1}^{t_2} \Pi(t)\mathrm{d}t\,, \tag{7.8}$$

which can be compared directly with Eqn.(2.11).

We are interested in how the negative current due to backflow would register in the distribution $\Pi(\tau)$ so we simplify Eqn.(7.7) with a weak measurement approximation,

$$\Pi(\tau) \approx 2V_0 \int_{-\infty}^{\tau} e^{2V_0(t-\tau)} \langle\psi_t|\hat{J}|\psi_t\rangle \tag{7.9}$$

where $|\psi_t\rangle = e^{-iH_0 t}|\psi_0\rangle$ and we have ignored the complex potential inside the bra-ket. This is the expected semiclassical result found elsewhere [13, 40]. We note that (7.9) is no longer positive semi-definite because here a negative current will result in a negative

distribution. This is due to taking the limit $V_0 \to 0$ inside the bra-ket but not the rest of the expression; however this does not matter for small V_0 and we will assume (7.9) is positive. This completes the model for a realistic arrival-time measurement from which the current can be derived either by deconvolution [40] or by taking a derivative. In principle this could be done experimentally and used to verify backflow via a negative current and flux.

Eqn.(7.9) has the form of a current smeared over the time interval which has been seen elsewhere in arrival-time models [18]. Smearing results in negative and positive current regions cancelling in the probability distribution $\Pi(\tau)$ which can manifest itself as a delay between the arrival of the wavepacket at the origin and its detection by the device. Yearsley et al [7] plot the measured probability Eqn.(7.9) for two values of V_0 alongside the numerically computed maximum bacfklow state; this illustrates how backflow leaves its trace in the time-smeared current. This plot is shown in Fig.(12). There is little difference between the backflow current and the smeared currents in the positive regions however the smeared current has become positive in the negative region. The behaviour at $t = \pm 1$ shows a discontinuous jump in the derivative of the smeared current which is clearly related to the singularity behaviour of the backflow current at these points. This is likely the backflow effect manifesting itself in the positive arrival-time distribution and points to a method of detecting backflow were the distribution to be recorded.

The above analysis dealt with the impact backflow has on the arrival-time distribution; does backflow also force us to alter our classical notion of detection and absorption? Muga et al sought to answer this question by studying how a backflow state interacts with a perfectly absorbing detector [11, 16]. Classically we consider a perfect particle detector to be almost point-like and detect all particles instantaneously, we will see that this notion cannot be fully applied in the quantum mechanical case.

Quantum mechanically a detector is considered to be a perfect absorber if its reflection and transmission rates vanish for a broad range of momenta Δ_p,

$$R(p) = T(p) = 0 \quad \forall p \in \Delta_p \tag{7.10}$$

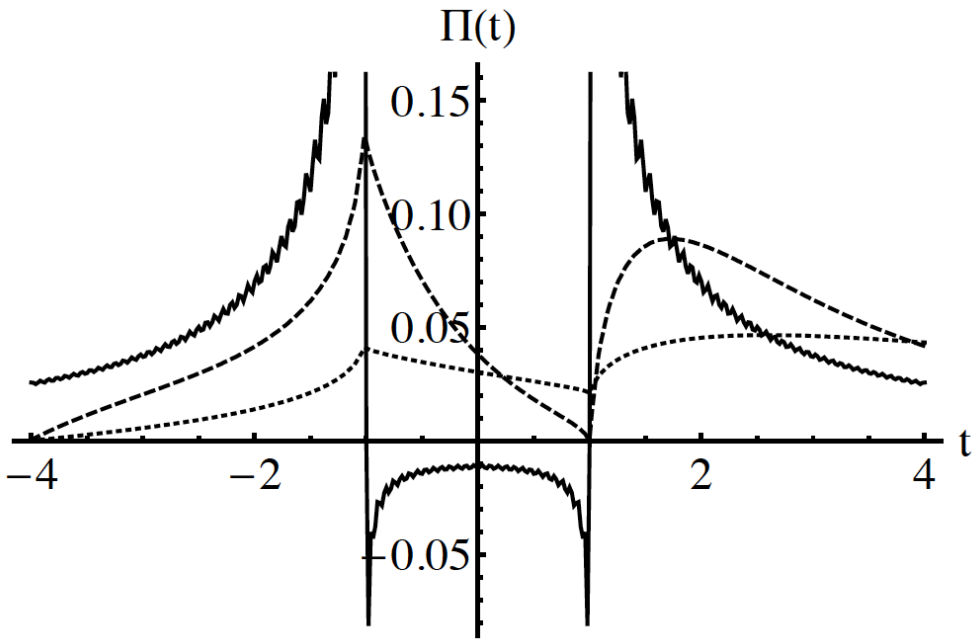

Figure 12: A plot of the time-smeared current for $V_0 = 0.5$ (dashed line) and $V_0 = 0.1$ (dotted line) and the maximal backflow current (solid line) [7].

where $R(p)$ and $T(p)$ are the reflection and transmission amplitudes respectively. We consider a detector with its front edge located at the origin modelled by a complex potential in the region $[0, L]$ [11]. Our free wavefunction without detector is φ and if the detector is present then the wavefunction is Ψ. Muga et al show that to the left of the detector, in the region $x \leq 0$, these two wavefunctions coincide [16], i.e.

$$\langle x|\varphi(t)\rangle = \langle x|\Psi(t)\rangle\,, \quad x \leq 0\,. \tag{7.11}$$

Moreover the currents are identical,

$$J_\varphi(x,t) = J_\Psi(x,t), \quad x \leq 0\,. \tag{7.12}$$

This is true regardless of whether or not the free current is positive. Hence for backflow states where $J_\varphi(0,t) < 0$, the detector 'returns' part of the probability that had entered $[0, L]$, without being absorbed, before the backflow period. This is not a reflection of the

particles from the detector, it is only a temporary emission of the probability which will eventually be fully absorbed [16]. If the detector was point-like and instantaneous, as in the classical case, then no norm could accumulate between $x = 0$ and $x = L$ without being absorbed[8]. Therefore the detector current at the origin $J_\Psi(0,t)$ could not match that of the backflow state as there would be no probability available to return. Essentially with a quantum mechanical detector we have a choice: if the detector is perfect (it eventually absorbs all particles) then it cannot be instantaneous as it must give back probability when backflow occurs; if the detector is instantaneous then the detector is necessarily imperfect because it cannot absorb all particles.

7.3 Detection using Bose-Einstein condensates

We saw above that a significant challenge to the experimental verification of backflow is the possibility of a direct measurement of the current. A recent paper by Palmero et al [20] attempts to do exactly that by relating the current to the particle density and suggesting a method for a density measurement using Bose-Einstein condensates (BEC). The appeal of BECs is twofold: they allow high levels of control and direction; and, remarkably, properties such as probability density and flux are properties of the individual particles in the condensate rather than statistical properties of the entire ensemble. This second feature is the crucial one in the present case, as it creates the possibility of measuring local properties such as the phase-gradient in a one-shot experiment.

We consider a 1-dimensional BEC with momentum centred around $p_1 > 0$. A Bragg pulse is applied which transfers momentum $q > 0$ to some atoms in the condensate creating a state with momentum $p_2 = p_1 + q$. The total normalised wavefunction is then,

$$\Psi(x,t) = \psi(x,t)[A_1 + A_2 e^{iqx+i\varphi}]\,, \tag{7.13}$$

[8]For a point-like detector $L \to 0$. Muga et al define an instant detector as one whose absorption rate equals the current, $-\mathrm{d}N(t)/\mathrm{d}t = J(0,t) \geq 0$ [16].

where $A_1 and A_2$ are the amplitudes of the two momentum states and φ is an arbitrary phase irrelevant for the experiment. Our initial wavepacket is,

$$\psi(x,t) = \phi(x,t)e^{i\eta(x,t)}\,, \tag{7.14}$$

where both ϕ and η are real-valued functions. In terms of the probability density, ρ_Ψ, the derived current is,

$$J_\Psi(x,t) = \frac{(\nabla\eta)\rho_\Psi + \frac{1}{2}q\left[\rho_\Psi + |\phi|^2(A_2^2 - A_1^2)\right]}{m} \tag{7.15}$$

From this we can derive an inequality for the negative current which corresponds to the density being below the critical level,

$$\rho_\Psi^{\text{crit}}(x,t) = \frac{q}{q + 2\nabla\eta(x,t)}|\phi(x,t)|^2(A_1^2 - A_2^2) \tag{7.16}$$

Hence we can experimentally detect backflow simply by measuring the density level and checking it is below the critical threshold. Our analysis applies to any wavefunctions of the form Eqn.(7.13) which is a fairly broad category including many of the wavefunctions discussed in this review.

How would the actual experiment proceed? We start with a BEC in a Gaussian initial state, $\psi_0(x)$, inside an harmonic trap which is suddenly shifted by length d where the condensate starts to oscillate. At $t = t_1$ when the condensate has reached momentum p_1, the trap is switched of and the condensate expands for a short time. Finally the Bragg pulse is applied and the BEC is in the form (7.13) with,

$$\phi(x) = \frac{1}{\sqrt{b(t)}}\psi_0\left[\frac{x - p_1 t/m}{b(t)}\right] \tag{7.17}$$

where $b(t)$ is a scaling parameter which evolves in time. By taking a snapshot of the interference pattern of this superposition, its minimum can be measured and compared to the

critical density. Regions with a density below the critical level will be undergoing backflow; this is shown in Fig.(13) for a ^{7}Li BEC which Palmero et al used to demonstrate their experiment.[9].

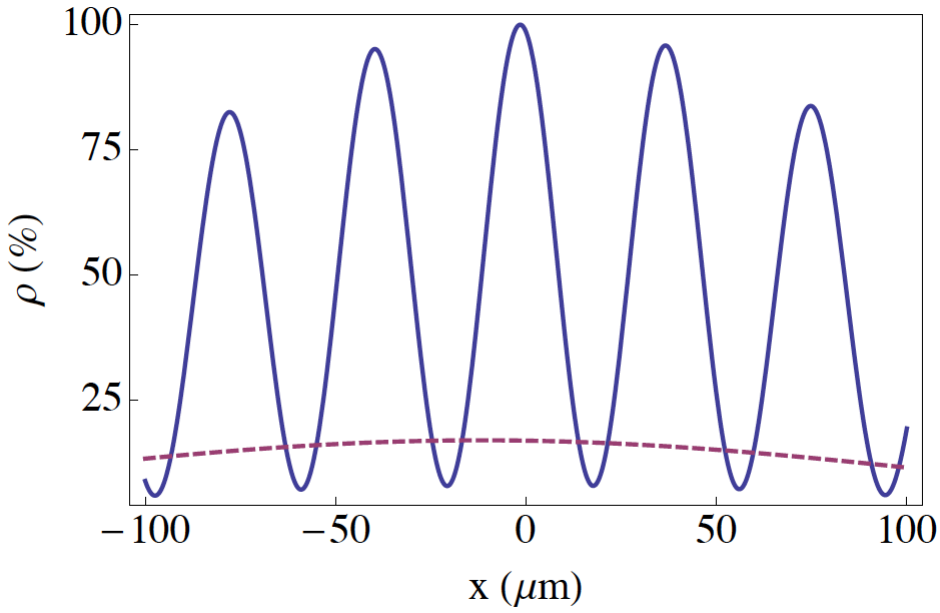

Figure 13: Critical density (dashed line) and actual density (solid line) for a ^{7}Li BEC. Backflow occurs in regions below the critical density. [20].

Presently, this is the only explicit method of detecting backflow that has been offered. There are issues concerned with the resolution of the imaging and calibration of the equipment however, these can both be overcome with current experimental technology [20]. The arrival-time detection models considered above offered insights into general time measurement problems which are relevant to more than just the backflow regime. However none of them attempted anything like a description of an experiment that could actually be performed. It is therefore appropriate to consider BECs as the best hope of experimentally verifying the backflow effect and we look forward to confirmation of this in the near future.

[9] ^{7}Li is a bosonic isotope of Lithium.

8. Interpreting backflow

Throughout this review there has been almost no discussion of how to interpret backflow or the physical mechanism by which it occurs. In this chapter we investigate how backflow results from the quantum mechanical formalism and explore unusual interpretations that can be applied. Due to its counterintuitive properties, backflow invites a variety of unorthodox explanations which can be both appealing and informative to explore.

8.1 The relationship with quantum mechanics

We want to understand what causes backflow and how to interpret the effect in the wider context of quantum mechanics. As a quantum effect with no classical counterpart, it is to be expected that any explanation of its cause must be deeply rooted in, and intrinsic to, the quantum mechanical description. Backflow can broadly be described as caused by two features integral to quantum mechanics: the uncertainty relations and superposition of states.

The uncertainty relations have been discussed throughout this paper, principally in sections 2.2 and 4.3, and we will recap their relevance here. The current operator Eqn.(2.8) is defined in terms of both the position operator and the momentum operator, two non-commuting observables. Although for positive momentum states position and momentum are both positive operators, their non-commutativity creates the possibility that $\hat{J}$ takes negative values. It is for this reason that backflow is described as originating in the uncertainty relations. That these relations do not obtain in classical mechanics provides

an appealingly simple reason for the non-existence of classical backflow. Strange commented on the depth of structure that exists within the uncertainty relations [10] and it is possible to view backflow as a manifestation of this. In principle, one could find versions of backflow which result from a broad range of non-commuting observables.

So far our examples of backflow states have all been superpositions; this is because the effect does not occur for single wave states. Negativity of the Wigner function is a necessary condition for backflow but it is also known to be an indicator of interference effects in the wavepacket [7]. By definition a single wave cannot have interference or a negative Wigner function hence superposition of states is equally a necessary condition for backflow. It is this detail which led Bracken and Melloy to describe backflow as a "kind of self-interference effect for quantum wavepackets" [9, p. 7]. One can view backflow at the origin as caused by some parts of the wavepacket having crossed the origin and some parts still lagging behind. The interference caused by this distribution in the probability density results in a brief negative current; overall however, the wavepacket moves forward. This can *roughly* been seen by viewing snapshots of the probability distribution of the backflow maximising state as it evolves over time (See Fig.(14)). At $t = 0$ the wavefunction is evenly distributed on both sides of the origin but at $t = 1$ there appears to be increased probability mass on the negative half of the x-axis.

It is clear that backflow can be entirely justified within the quantum mechanical framework and is not some relic of a faulty description, but in fact intrinsic to the quantum world. This leads us to question whether something can be learned from backflow with regard to quantum mechanics. Eveson et al suggest that "backflow provides a nice illustration of the inadequacy of the phase velocity alone to predict the motion of a wavepacket" [5, p.4]. Indeed, we saw in sections 3.3 and 3.4 that Berry's analysis of the effect concentrated on the phase gradient rather than the current. When a state is written in the form Eqn.(3.17), the phase gradient corresponds to the *local* wavenumber and below Eqn.(8.1) establishes the *local* mean velocity. We know that in standard quantum mechanics local

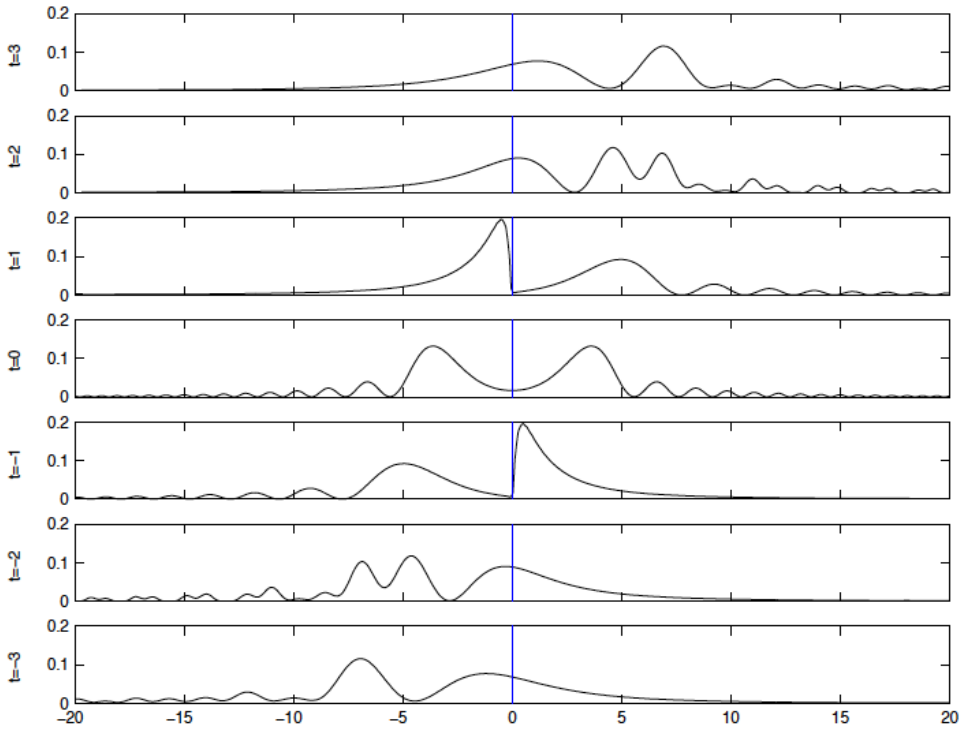

Figure 14: A plot of the position probability density for the backflow maximising state (Fig.(8)) in the range $[-20, 20]$ for intervals of t [6].

realism — the notion that objects have pre-determined properties influenced only by their surroundings — is rejected [41]. Measurement takes a fundamental position in quantum theory for we understand properties as having values only upon measurement. Since the local wavenumber cannot be directly measured it is entirely consistent for it to have an unexpected, negative, value. Exactly the same principle lies behind the phenomenon of superoscillations in which the local wavenumber exceeds that of its components which satisfy the Helmholtz equation [25]. We must be careful not to speak of extant local properties since such properties do not actually exist[10]. Although backflow seems to imply that the particle is locally travelling backwards, it is really only the probability wave (a non-physical entity) which is. Backflow is a reminder that the global properties of the state do not uniquely determine every aspect of the dynamics.

[10] As we will see below Bohmian theory accepts the existence of local properties.

For the rest of this chapter we examine unusual interpretations that are applied in the quantum mechanical setting and have particular relevance to the case of backflow.

8.2 The Dirac velocity

It is well known that velocity holds a different status among particles described by the Dirac equation to that of their bosonic counterparts. Dirac noticed at an early stage that his equation and framework allowed one to interpret velocity and momentum as distinct concepts, not simply related by the equation $p = mv$ [42]. Remarkably, there exists a velocity operator which commutes with both the position and momentum operators [43] and whose eigenvalues are $\pm c$. This would seem to imply that Dirac particles travel at the speed of light regardless of their mass. This is in contrast to integer-spin particles whose velocity can be anywhere in the range $[-c, c]$. However, a measured velocity of $\pm c$ would only arise if the system is actually in an eigenstate of the velocity operator; for arbitrary states, the velocity expectation value will usually be less than c [43]. Additionally, there is the Zitterbewegung phenomenon, first discovered by Schrödinger [44], during which an electron rapidly oscillates about its median position near to the speed of light [45]. These features of a Dirac particle suggest that there may be curious ways to interpret backflow in relation to the particles velocity which are not available in the spinless case.

Bracken and Melloy are the only authors to investigate backflow for a relativistic Dirac particle [9] and, consequently, they are the only authors to offer any interpretation of what backflow physically means in that case. Their focus is on the independence of velocity and momentum operators. The velocity operator for a Dirac particle can be defined as $\hat{\dot{x}} = c\sigma_1$ while the momentum operator has its usual form. One can also define the local mean velocity[11] ,

$$v(x,t) = \frac{J(x,t)}{\rho(x,t)} \tag{8.1}$$

which must clearly take the same sign as $J(x,t)$ due to the positivity of $\rho(x,t)$. Bracken and

[11] This definition of local mean velocity applies to both Dirac and Schrödinger particles and thus all the examples in this study.

Melloy argue that, due to the commutativity of $\hat{x}$ and $\hat{\hat{x}}$, it makes sense to consider $v(x,t)$ as the local expectation value of the velocity operator. Hence, the negativity of $J(x,t)$ (and therefore $v(x,t)$) is directly a consequence of the velocity operator having positive *and* negative eigenvalues even when the momentum is strictly positive. It is likely this argument which led Berry to suggest that during backflow Dirac particles 'literally...masquerade as antiparticles' [23, p.2]. The implication is that a period of negative current for an electron is equivalent to positive current for a positron. Bracken and Melloy suggest that an experimental verification of Dirac backflow would equally be a verification of the independence of velocity and momentum.

We do not believe that this interpretation prevails under scrutiny. The primary obstacle to accepting this interpretation of the backflow effect is that, at best, it applies to only half of all possible cases. Only one example in this review considered a Dirac particle; the rest, involving spinless particles, remain entirely unexplained because their velocities and momenta are not considered independent. It is a basic tenet of science that one should accept only those explanations that apply to the broadest possible range of cases [46]. The above explanation of backflow clearly fails to satisfy that requirement. Were the interpretation of backflow in the bosonic case to exclude spin-1/2 particles then Bracken and Melloy's proposal would be more acceptable (although one would still have to explain why two separate effects, entirely independent in cause, are indistinguishable in outcome). The second problem with this interpretation is that the distinction between velocity and momentum only applies in a limited number of circumstances. In a comprehensive study of Dirac velocity, Davies has shown that a divergence in the status of velocity between spinless and spin-1/2 particles only occurs in the limit $m \to 0$ [43]. Under normal circumstances, a velocity measurement for a relativistic Dirac particle with positive momentum will record a value in the range $[0, c]$. Thus, we see that the negativity of $J(x,t)$, and $v(x,t)$ along with it, is not explained by the possibility of the velocity and momentum operators returning eigenvalues with opposite signs.

8.3 Bohmian mechanics

Bohmian mechanics provides an easy explanation of the backflow effect for those who subscribe to the theory. Before examining this in detail, we must first introduce some basic concepts of Bohmian theory.

Consider an electron propagating in 1-dimension; Bohmian mechanics postulates that it is both an actual point-like particle and a pilot-wave $\psi(x,t)$ which guides the particle's motion[12] . The electron has a well defined position $x(t)$ and velocity $v(t)$ at all times and is governed by the following equation of motion,

$$v(x,t) \equiv \frac{\mathrm{d}x(t)}{\mathrm{d}t} = \frac{J(x,t)}{\rho(r,t)} \tag{8.2}$$

Notice that the right hand side is exactly the relation we defined above as the 'local mean velocity', Eqn.(8.1); this correspondence makes sense because in Bohmian theory the electron is considered to have well defined local properties. $\psi(x,t)$ is still the solution to the relevant equation (either Schrödinger or Dirac) and we posit that $\rho(x,t)\mathrm{d}x$ is the probability that the particle component of the electron is in the region $\mathrm{d}x$. This need only be true at $t = 0$ because the continuity equation (2.3) ensures that it is true at all later times [15].

Notice measurement plays no role in this interpretation; the particle *is* in a specific location rather than *is found* in a specific location. However, experiments involving measurement at a chosen instant of time will produce no discernible difference between orthodox and Bohmian theory. Quantum mechanical uncertainty is introduced only in the uncertainty of the electrons initial position which causes uncertainty at all later times. Eqn.(8.2) means that any particle arriving at $x = 0$ with $J(0,t) > 0$ must come from the left and those arriving with $J(0,t) < 0$ must come from the right; in a sense this corresponds to our classical intuition. Hence, we write the arrival-time distribution in a way that makes

[12]The example is equally applicable to a photon or other quantum particle however because of the peculiar distinction between point-particle and wave in Bohmian theory it is confusing to talk of a 'quantum particle that is both a point-particle and a wave' so instead I refer here to an electron.

this explicit,

$$\Pi(t) = \Pi_+(t) + \Pi_-(t) \tag{8.3}$$

where the subscripts + and - correspond to arrival from the left and right respectively. The left and right distributions are defined as,

$$\Pi_\pm(t) = \pm N J_\pm(x,t) \geq 0 \tag{8.4}$$

with

$$N^{-1} = \int_0^\infty [J_+(x,t) - J_-(x,t)]\mathrm{d}t \tag{8.5}$$

and

$$J_\pm(x,t) = J(x,t)\theta[\pm J(x,t)]\,. \tag{8.6}$$

The paradoxical or counterintuitive nature of backflow lies in the fact that a particle arriving at $x = 0$ from the left seems to have an increasing probability of staying in the region $[-\infty, 0]$. However, in Bohmian mechanics the negativity of the current means that the particle *must* be arriving from the right which no longer seems problematic. Rather, it has replaced the paradox of a particle travelling in an opposite direction to its momentum with the strange notion that a free particle travelling from the left has changed direction mid-flight and is now approaching the origin from the right. Yet this unusual idea is easily explained in Bohmian mechanics: the particle is not actually free but at all times controlled by its guiding wave which has directed it to change direction.

Thus, Bohmian mechanics provides a description of the actual physical mechanism by which backflow occurs. It is not the point of this review to discuss the merits of Bohmian theory but we would argue that the easy incorporation of backflow into the theory is a mark in its favour. Of course this feature would not be enough to convince most people to accept the theory and it is not without need of additional work to render the explanation more convincing. In particular, we saw in section 7.2 that the arrival-time distribution of a backflow state show discontinuous jumps in the derivative of the current at the points

when backflow starts and ends. This corresponds to a discontinuous change in the particle's velocity using Eqn.(8.2); it is then incumbent upon the Bohmian theorist to explain how the pilot-wave causes a discontinuous, rather than smooth, change in the particle's direction of travel.

8.4 Negative probabilities

Negative probabilities can be a difficult concept to process; our intuition rejects the idea that there can be less than no chance of something happening. However, negative probabilities and the broader class of quasiprobabilities[13] are often found in physics and mathematics which suggests we should seek a way to interpret them. In quantum mechanics quasiprobabilities are often found when non-commuting observables are involved and they are used in a similar manner to probabilities [28]. Feynman argued that despite their seemingly nonsensical nature they are mathematically well defined and can be used as a calculational tool or to extract information about a system [27]. Is there a way to make sense of backflow through the use of negative probabilities?

Bracken and Melloy argue that backflow is best described as the positive flow of negative probability rather than the negative flow of positive probability [4]; the two, of course, are mathematically equivalent. In this view, the probability current is always flowing in the same direction but during backflow intervals the probability that flows is negative. It is unclear what the advantage of this interpretation is nor what it would mean physically. We saw that the Wigner function was rejected as a probability distribution due to its susceptibility to negative values, even though if one restricts to hermitian observables then any probability calculated using the Wigner function will be in the range $[0, 1]$. Halliwell and Yearsley have shown that quasiprobabilities can be split into two qualitatively different types: viable and nonviable. Viable quasiprobabilities have positive marginals which match those of a standard probability, whereas nonviable quasiprobabilities do not [28].

[13] Quasiprobabilities are probabilities which lie outside the range $[0, 1]$.

Viable quasiprobabilities are qualitatively similar to probabilities and can be similarly interpreted or, perhaps, interpreted as their matching positive probability, while nonviable quasiprobabilities lead to non-physical results. We assume negative backflow probabilities would be viable as they can readily be exchanged for positive probabilities flowing in the opposite direction, however, this is currently unknown. Halliwell's work suggests there might be a way to make sense of interpreting backflow as the flow of negative probability; but, until this is thoroughly investigated there appears to be no advantage to this interpretation.

8.5 Summary

We have seen diverse interpretations that can be applied to backflow with various levels of success. The independence of the Dirac velocity and momentum seems the least successful of the available interpretations in no small part due to its limited applicability. For those who subscribe to the view, Bohmian mechanics offers a convenient description of how backflow occurs, though it is not without need of improvement. Were negative probabilities to become an accepted concept in quantum mechanics then backflow would surely be a scenario in which they would be particularly relevant. However, until they are in common use there seems little motivation to use them rather than negatively directed positive probabilities. It is, as one would expect, within typical quantum mechanics and its intrinsic features of non-commutativity and superposition that we find the most legitimate explanations for, and interpretations of, backflow. The non-classical effect can be directly traced back to its quantum origins which provide a simple explanation for how the effect occurs.

9. Conclusion

9.1 Future work

Backflow has largely been ignored or unexplored by most physicists. As a result there remain a number of open questions and problems to resolve. We will highlight here some of the issues we think are most pressing and which have a hope of being assayed in the future.

The most immediate issue is finding an analytic solution to the eigenvalue problem Eqn.(2.15). Penz et al comment that it remains an open question whether or not there actually is a backflow eigenvalue which corresponds to $-c_{bm}$ [6]. Finding an analytic maximum backflow state which solves Eqn.(2.15) would confirm that there is as well as providing insight into the effect itself. Yearsley et al were partially successful in their search for the state and their findings are encouraging [7]. We believe that if continued effort is made then an analytic solution will soon be found. A related issue concerns eigenstates which satisfy Eqn.(2.15) with eigenvalues less negative than $-c_{bm}$. Halliwell et al provided an exhaustive class of backflow states [22] but it is extremely general and it would be worthwhile to study more specific classes of analytic solutions were they to exist.

It is impressive how easily Strange [10] was able to find an entirely new type of backflow which suggests that it is a worthwhile line of inquiry. The existence of an enormous number of uncertainty relations indicates that there may be many other types of backflow waiting to be found. Their discovery could lead to simpler methods of experimental verification than those currently proposed and thus hasten confirmation of the effect. It is also

of significance to investigate what other backflow limits exist. In particular a spacetime bound is worth exploring and the possibility that classes of backflow states are subject to stricter conditions than the general case.

Experimental verification is of course an aim that must be achieved and now that Plamero et al have suggested a workable scheme using Bose-Einstein condensates [20] we see no reason for this not to be resolved promptly. An experiment will likely raise as many questions as it answers and is, therefore, crucial in order to understand more about backflow and backflow states than the theoretical concerns raised here. Examples of issues that could be explored are the (unusual) mass dependence of backflow for a relativistic Dirac particle and the lifetime of backflow periods in real-life systems.

9.2 Summary

This review aimed to provide a complete description of the backflow effect and all relevant features and concerns. In chapter 2 we introduced the effect and the necessary tools and concepts for analysis. We showed that it is possible for states with only positive momentum located in the half-space $x < 0$ to temporarily increase the probability of staying in $x < 0$. We set up an eigenvalue problem which allowed us to calculate the maximum amount of probability flux that can flow backwards in any time interval. This maximal eigenvalue, c_{bm}, has an accepted value of 0.038452 and is dimensionless and independent of any parameters.

In chapter 3 we explored how c_{bm} could be related to a temporal bound which limits the duration of the backflow effect. A spatial bound was also introduced which related the area of the back-flowing region to the size of the current. Berry's work proposed the concept of a backflow measure, which is a way to determine what fraction of the axis is undergoing backflow. This was found to be dependent on the spread of component momenta and strong backflow was shown to occur for highly correlated momenta. An equivalence between backflow and superoscillations — another quantum effect — was

made explicit.

Chapter 4 investigated the types of systems that could exhibit the effect. It was shown that backflow can occur both in opposition to a force and for a relativistic Dirac particle. This suggests that backflow might be possible in a wide array of situations. Both cases resulted in the amount of backflow becoming parameter dependent and this dependence was discussed with particular interest in the unusual mass behaviour. A new type of backflow in which the state's *angular* momentum is locally in the opposite direction to the component angular momenta was demonstrated. We raised the possibility of a broad range of backflow effects.

In chapter 5 we showed how negativity of the Wigner function is a necessary but insufficient condition for backflow. We then explored the range of states so far shown to exhibit the effect. Superpositions of Gaussians proved to be particularly good at producing large amounts of backflow while plane waves were not. An exhaustive class of backflow states were discussed and in once example 41% of the maximum possible negative flux was produced. We investigated the maximal backflow state and an attempt to approximate it with analytic functions. These were not successful at matching the behaviour near the start and finish of the backflow interval, however, they were able to produce 72% of the maximum flux.

Chapter 6 briefly examined backflow's classical limit (or lack thereof) and how to restore it. We saw that by making our backflow system more realistic, a classical limit was naturally introduced. We looked in detail at one method of doing this using quasi-projectors which model how projections are done in real life experiments. The negative eigenvalues of Eqn.(2.15) were found to tend to zero as we took our classical limit, while the positive (non-backflow) eigenvalues were largely unchanged.

The details of experimental verification were reviewed in chapter 7. We discussed theoretical issues related to the arrival-time problem and how this is connected with backflow. We then looked in detail at a theoretical detection model using complex potentials and showed how we got a smeared current in which backflow left its signature by discon-

tinuous changes in the current derivate. The notion of a perfectly absorbing detector was scrutinised and shown to be wanting in the quantum mechanical case. We concluded by detailing a realistic method for detecting backflow by checking whether the density of a Bose-Einstein condensate goes below a critical threshold.

Our last chapter focused on how to interpret backflow. Various unusual interpretations were discussed; in particular, Bohmian mechanics easily incorporated the backflow effect with into its theory. However it was clear that the easiest and most informative way to understand backflow was through orthodox quantum mechanics and the concepts of uncertainty and superposition.

Finally, we discussed the direction which future research should take. There is still much work to be done.

Bibliography

[1] G R Allcock. ``The time of arrival in quantum mechanics II. The individual measurement''. In: *Annals of Physics* 53.2 (1969), pp. 286–310. doi: 10.1016/0003-4916(69)90252-8.

[2] G R Allcock. ``The time of arrival in quantum mechanics I. Formal considerations''. In: *Annals of Physics* 53.2 (1969), pp. 253–285. doi: 10.1016/0003-4916(69)90251-6.

[3] G R Allcock. ``The time of arrival in quantum mechanics III. The measurement ensemble''. In: *Annals of Physics* 53.2 (1969), pp. 311–348. doi: 10.1016/0003-4916(69)90253-X.

[4] A J Bracken and G F Melloy. ``Probability backflow and a new dimensionless quantum number''. In: *Journal of Physics A: Mathematical and General* 27.6 (1994), pp. 2197–2211. doi: 10.1088/0305-4470/27/6/040.

[5] SP Eveson, CJ Fewster, and R Verch. ``Quantum inequalities in quantum mechanics''. In: *Annales Henri Poincaré* 6.1 (2005), pp. 1–30. doi: 10.1007/s00023-005-0197-9. arXiv:0312046v1.

[6] M Penz et al. ``A New Approach to Quantum Backflow''. In: *Journal of Physics A: Mathematical and General* 39.2 (2006), pp. 423–433. doi: doi:10.1088/0305-4470/39/2/012. arXiv:0511109 [quant-ph].

[7] J M Yearsley et al. ``Analytical examples, measurement models, and classical limit of quantum backflow''. In: *Physical Review A* 86.4 (2012), p. 42116. doi: 10.1103/PhysRevA.86.042116. arXiv:1202.1783v5.

[8] G.F. Melloy and A.J. Bracken. ``The velocity of probability transport in quantum mechanics''. In: *Annalen der Physik* 7.7-8 (1998), pp. 726–731. doi: 10.1002/(SICI)1521-3889(199812)7:7/8<726::AID-ANDP726>3.0.CO;2-P.

[9] GF Melloy and AJ Bracken. ``Probability backflow for a Dirac particle''. In: *Foundations of physics* 28.3 (1998), pp. 505–514. doi: 10.1023/A:1018724313788.

[10] P Strange. ``Large quantum probability backflow and the azimuthal angle–angular momentum uncertainty relation for an electron in a constant magnetic field''. In: *European Journal of Physics* 33.5 (2012), pp. 1147–1154. doi: 10.1088/0143-0807/33/5/1147.

[11] JG Muga, JP Palao, and CR Leavens. ``Quantum arrival time measurement and backflow effect''. In: *Arxiv preprint* (1998). arXiv:9803087.

[12] Y. Aharonov et al. ``Measurement of time of arrival in quantum mechanics''. In: *Physical Review A* 57.6 (1998), pp. 4130–4139. doi: 10.1103/PhysRevA.57.4130.

[13] J. J. Halliwell and J. M. Yearsley. ``Arrival times, complex potentials, and decoherent histories''. In: *Physical Review A* 79.6 (2009). doi: 10.1103/PhysRevA.79.062101.

[14] J G Muga, R Sala Mayato, and Í L Egusquiza, eds. *Time in Quantum Mechanics - Vol. 1*. Berlin: Springer, 2008. doi: 10.1007/978-3-540-73473-4.

[15] JG Muga and CR Leavens. ``Arrival time in quantum mechanics''. In: *Physics Reports* 338.4 (2000), pp. 353–438. doi: 10.1016/S0370-1573(00)00047-8.

[16] JG Muga, JP Palao, and CR Leavens. ``Arrival time distributions and perfect absorption in classical and quantum mechanics''. In: *Physics Letters A* 253.1-2 (1999), pp. 21–27. doi: 10.1016/S0375-9601(99)00020-1.

[17] J. M. Yearsley. ``Quantum arrival time for open systems''. In: *Physical Review A* 82.1 (2010), p. 012116. doi: 10.1103/PhysRevA.82.012116.

[18] J. M. Yearsley et al. ``Quantum arrival and dwell times via idealized clocks''. In: *Physical Review A* 84.2 (2011), p. 022109. doi: 10.1103/PhysRevA.84.022109.

[19] J G Muga, S Brouard, and D Macías. ``Time of Arrival in Quantum Mechanics.pdf''. In: *Annals of Physics* 240 (1995), pp. 351–366. doi: 10.1006/aphy.1995.1048.

[20] M Palmero et al. ``Detecting quantum backflow by the density of a Bose-Einstein condensate''. In: *Physical Review A* 87.5 (2013), pp. 1–5. doi: 10.1103/PhysRevA.87.053618. arXiv:1302.3373v2.

[21] JM Yearsley and JJ Halliwell. ``An introduction to the quantum backflow effect''. In: *Journal of Physics: Conference Series* 442.Conference 1 (2013). doi: 10.1088/1742-6596/442/1/012055. arXiv:1301.4893v1.

[22] JJ Halliwell et al. ``Quantum Backflow States from Eigenstates of the Regularized Current Operator''. In: *arXiv preprint:1309.2909* (2013). arXiv:1309.2909v1.

[23] M V Berry. ``Quantum backflow, negative kinetic energy, and optical retro-propagation''. In: *Journal of Physics A: Mathematical and Theoretical* 43.41 (2010), p. 15. doi: 10.1088/1751-8113/43/41/415302.

[24] M V Berry. ``Faster than fourier''. In: *Quantum Coherence and Reality; in celebration of the 60th Birthday of Yakir Aharonov*. Ed. by J S Anandan and J L Safko. Singapore: World Scientific, 1994, pp. 55–65.

[25] M V Berry and M R Dennis. ``Natural superoscillations in monochromatic waves in D dimensions''. In: *Journal of Physics A: Mathematical and Theoretical* 42.2 (2009), p. 022003. doi: 10.1088/1751-8113/42/2/022003.

[26] M V Berry and S Popescu. ``Evolution of quantum superoscillations and optical superresolution without evanescent waves''. In: *Journal of Physics A: Mathematical and General* 39.22 (2006), pp. 6965–6977. doi: 10.1088/0305-4470/39/22/011.

[27] Richard Feynman. ``Negative Probability''. In: *Quantum Implications: Essays in honour if David Bohm*. Ed. by B.J. Hiley and F. David Peat. 1st. 1987.

[28] J. J. Halliwell and J. M. Yearsley. ``Negative probabilities, Fine's theorem, and linear positivity''. In: *Physical Review A* 87.2 (2013). doi: 10.1103/PhysRevA.87.022114.

[29] M Ruggenthaler, G Grübl, and S Kreidl. ``Times of arrival: Bohm beats Kijowski''. In: *Journal of Physics A: …* 38.39 (2005), pp. 1–9. doi: 10.1088/0305-4470/38/39/010. arXiv:0504185v1.

[30] J G Muga, A Ruschhaupt, and A del Campo, eds. *Time in Quantum Mechanics - Vol. 2*. Berlin: Springer, 2009. doi: 10.1007/978-3-642-03174-8.

[31] M Bordag, U Mohideen, and V M Mostepanenko. ``New developments in the Casimir effect''. In: *Physics Reports* 353.1–3 (2001), pp. 1–205. doi: 10.1016/S0370-1573(01)00015-1.

[32] Yakir Aharonov, David Z Albert, and Lev Vaidman. ``How the result of a measurement of a component of the spin of a spin-1/2 particle can turn out to be 100''. In: *Physical Review Letters* 60.14 (1988), pp. 1351–1354. doi: 10.1103/PhysRevLett.60.1351.

[33] L Vaidman. ``Emergence of Weak Values''. In: *Arxiv preprint* (1996), pp. 1–12. arXiv: 9607023v1 [arXiv:quant-ph].

[34] Yakir Aharonov and Daniel Rohrlich. *Quantum Paradoxes*. 1st. Wiley-VCH, 2005.

[35] Y Aharonov et al. ``Measurements, errors, and negative kinetic energy.'' In: *Physical review. A* 48.6 (1993), pp. 4084–4090. doi: 10.1103/PhysRevA.48.4084.

[36] Lev Landau and Evgeny Lifshitz. *Quantum Mechanics*. 3rd. Oxford: Butterworth-Heinemann, 2003.

[37] Lajos Diósi and Claus Kiefer. ``Exact positivity of the Wigner and P-functions of a Markovian open system''. In: *Journal of Physics A: Mathematical and General* 35.11 (2002), pp. 2675–2683. doi: 10.1088/0305-4470/35/11/312.

[38] J M Yearsley and J J Halliwell. ``Quantum arrival time formula from decoherent histories''. In: *Physics Letters A* 374.2 (2009), p. 154. doi: 10.1016/j.physleta.2009.10.077.

[39] J J Halliwell and J M Yearsley. ``On the relationship between complex potentials and strings of projection operators''. In: *Journal of Physics A: Mathematical and Theoretical* 43.44 (2010), p. 445303. doi: 10.1088/1751-8113/43/44/445303.

[40] J A Damborenea et al. ``Measurement-based approach to quantum arrival times''. In: *Physical Review A* 66.5 (), p. 52104. doi: 10.1103/PhysRevA.66.052104.

[41] J S Bell. *Speakable and unspeakable in quantum mechanics*. 1st. Cambridge: Cambridge University Press, 1987.

[42] Paul A M Dirac. *The Principles of Quamtum Mechanics*. 4th. Oxford: Oxford University Press, 1958.

[43] PCW Davies. ``Measurement of the velocity of a Dirac particle''. In: *Journal of Physics A: Mathematical and General* 19.11 (1986), pp. 2115–2121. doi: 10.1088/0305-4470/19/11/020.

[44] E Schrödinger. ``Über die kräftefreie Bewegung in der relativistischen Quantenmechanik''. In: *Sitzungber. Preuss. Akad. Wiss. Phys.-Math. Kl.* 24 (1930), p. 418.

[45] D Hestenes. ``The zitterbewegung interpretation of quantum mechanics''. In: *Foundations of Physics* 20.10 (1990), pp. 1213–1232. doi: 10.1007/BF01889466.

[46] M Curd, J A Cover, and C Pincock. *Philosophy of Science: The Central Issues*. 2nd. W W Norton & Company Incorporated, 2012.